

¹³C NMR ANALYSIS OF TRIGLYCERIDE FATTY ACID ENRICHMENT FROM ¹³C-ENRICHED LIPOGENIC SUBSTRATES

Miguel Fernando Ferreira Navarro



Miguel Fernando Ferreira Navarro

¹³C NMR ANALYSIS OF TRIGLYCERIDE FATTY ACID ENRICHMENT FROM ¹³C-ENRICHED LIPOGENIC SUBSTRATES

Dissertação no âmbito Mestrado em Bioquímica orientada pelo Doutor John Griffith Jones e apresentada ao Departamento de Ciências da Vida.

Agosto de 2018

Acknowledgments

To my whole family, with special attention to my younger brother Abel who did not use his personal computer to lend during all this work and, to my parents, António and Piedade and my grandmother, Encarnação, who have always believed in me and have invested in my education, both through their time and knowledge and through the money made available.

I'm also very grateful to my girlfriend, Beatriz, whom I could not give the proper attention and spend my time on.

A very special thanks to my close friends, who encouraged me to work on my thesis and who never abandoned me during this process.

I'm also eternally grateful to my supervisor Dr. John, who always had a minute for me and to explain some matter to me and to guide me throughout this project. Also, to my co-supervisor Dr. Rui who taught me how to work with the NMR machines and who indicated Dr. John to be my supervisor and was always available to me when I needed something

Also, a very special thanks to the guys from Intermediary Metabolism group, Ludgero, João, Ivan, Mariana, J. Rito, Cristina, Getachew and Emanuel who always helped me in everything and in discussion my results.

And finally, to the CNC, in particular the UC Biotech which made possible my work, and also to the UC for the NMR facilities.

Thanks to all.

Abstract

Lipids have central roles in cell structure and energy generation, there is high interest in analysis of the different types of lipids in the cell the study of all this matter is referred to as lipidomics, which is often regarded as a branch of metabolomics. Through a quantitative and qualitative analysis of lipids they can tell part of the history behind a disease or healthy organism. In the current work 1D ¹³C Nuclear Magnetic Spectroscopy gives a detailed insight of the triglycerides fatty acid composition and positions, using the natural abundance of the ¹³C isotope. We applied this approach to resolve the contributions of different fatty acids to triglycerides recovered from mouse visceral adipose tissues. Also, as a first step towards combining lipidomic analyses with measurements of fatty acid ¹³C-enrichment from ¹³C-enriched precursor substrates, we also identified and measured ¹³C-¹³C-spin-spin coupling constants from glyceryl trioleate. ¹³C-¹³C-spin-spin coupled signals from oleate were successfully identified in triglyceride fatty acids obtained from a mouse that had been fed with [U-¹³C]glucose.

Keywords: Lipidomics, Nuclear Magnetic Resonance (NMR), Triglycerides, Fatty acids, Positional fatty acids composition ¹

¹ Abbreviations: NMR, nuclear magnetic resonance; NAFLD, non-alcoholic fatty liver disease; GC-MS, gas chromatography-mass spectroscopy; AT, adipose tissue; FFA, free fatty acids; FID, free induction decay; NOE, nuclear Overhauser effect; FAME, fatty acid methyl ester; TLC, thin layer chromatography.

I. Index

1	Lipids as biomolecules	4
2	Lipids as a class	5
2.1	Lipids classification and nomenclature	5
2.2	Fatty acyls	6
2.2.1	Fatty acids	6
2.2.1.1	Structure and Nomenclature	7
2.2.1.2	Hepatic fatty acid Metabolism	9
2.2.1.2.1	Fatty acid uptake	10
2.2.1.2.2	Fatty acid Synthesis	10
2.2.1.2.3	Fatty acids desaturation and elongation	10
2.3	Glycerolipids	11
2.3.1	Triacylglycerol Metabolism	13
2.3.1.1	Digestion of dietary triglycerides	13
2.3.1.2	Triglycerides synthesis	13
3	NMR analysis of lipids	15
3.1	Overview of NMR in molecular structure analysis	15
	¹ H NMR spectroscopy of lipids	16
	¹³ C NMR spectroscopy of lipids	17
4	Materials and Methods	20
4.1	Reagents and Materials	20
4.2	Standard Preparation	21
4.3	Thin Layer Chromatography	21
4.4	Biological Samples	21
4.5	NMR spectroscopy	22
5	Results and Discussion	23
5.1	NMR Assignments	23
5.1.1	¹³ C NMR	23
5.2	Standard mixture quantitative analysis	29

¹³C NMR analysis of triglyceride fatty acid enrichment from ¹³C-enriched lipogenic substrates

5.3	Biological samples	34
5.4	Detection of ¹³ C- ¹³ C-coupling and measurement of ¹³ C- ¹³ C coupling constants	39
6	Conclusions	42
7	References	43
	Annex I.....	46
	Annex II.....	47

1 Lipids as biomolecules

Lipid, etymologically derived from the Greek word *lipos* which means “fat “, refers to a family of biomolecules that that can be roughly defined as being soluble in non-polar solvents, and which are hydrophobic or amphiphilic. Due to their characteristics these biomolecules have a vital role in numerous pathways including energy storage, structural support acting as part of the cell membranes, protection, and even signaling.

In terms of abundance, lipids constitute nearly 50% of the mass from the majority of animal cell membranes (4 Alberts, B. et al. (2007) *Molecular Biology of the Cell*. Garland Science).

A number of diseases are closely related with fat metabolism such as NAFLD (non-alcoholic fatty liver disease) and Type 2 diabetes. NAFLD is defined as an accumulation of fat in the hepatocytes in the absence of significant alcohol intake and it represents a major economic burden in European countries. The prevalence of this disease in Europe it's 2-44% for general population and 42.6-69.5% in people with type 2 diabetes, depending on the country (Blachier, Leleu, Peck-radosavljevic, Valla, & Roudot-thoraval, 2013).

Due to its central roles in cell structure and energy generation, there is high interest in analysis of the different types of lipids in the cell the study of all this matter is referred to as lipidomics, which is often regarded as a branch of metabolomics. Although many analytical methodologies such as GC-MS and ¹³C NMR were developed in 70's and 80's to identify and quantify different lipid species, their systematic application to study lipid metabolism in healthy and disease states has only begun in the last decade or so.

2 Lipids as a class

As for many other components of biological tissues, lipids are mainly composed of atoms of carbon, hydrogen and oxygen. The key aspect of this class of molecules is their solubility in organic solvents. This feature, in addition to the presence of long hydrocarbon, chains allows us to define lipids (see Figure 1).

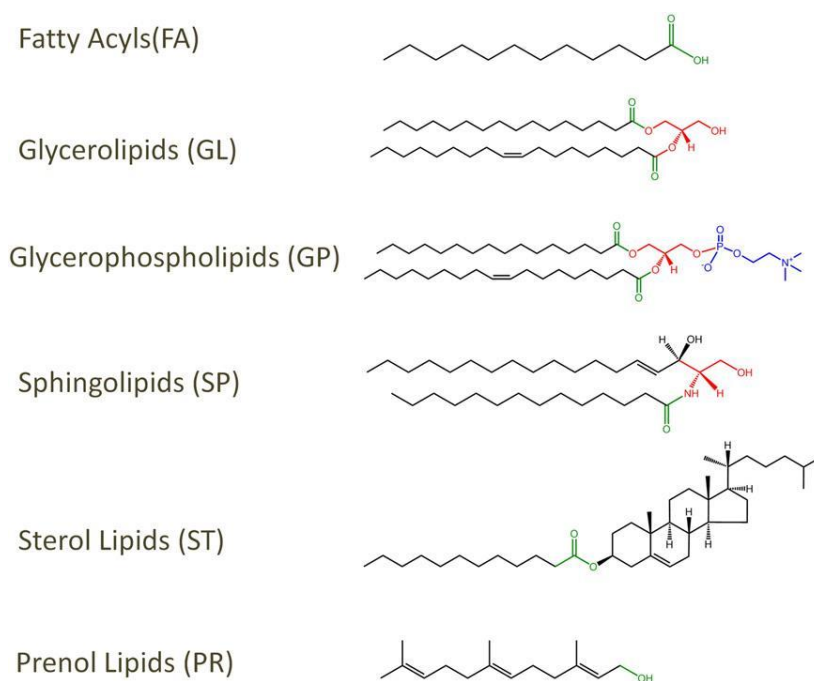


Figure 1: Lipids classes (Fahy, Cotter, Sud, & Subramaniam, 2011)

2.1 Lipids classification and nomenclature

The major building blocks of biological lipids are ketoacyl and isoprene groups therefore all lipids result from a condensation of ketoacyl and/or isoprene groups (Fig. 2). Having this in mind LIPID MAPS consortium, founded in 2003, have suggested a lipid nomenclature for lipids which separates this type of biomolecules in eight major groups: fatty acyls, glycerolipids, glycerophospholipids, sphingolipids, saccharolipids, polyketides, sterol lipids and prenyl lipids (Fahy, Cotter, Sud, & Subramaniam, 2011).

^{13}C NMR analysis of triglyceride fatty acid enrichment from ^{13}C -enriched lipogenic substrates

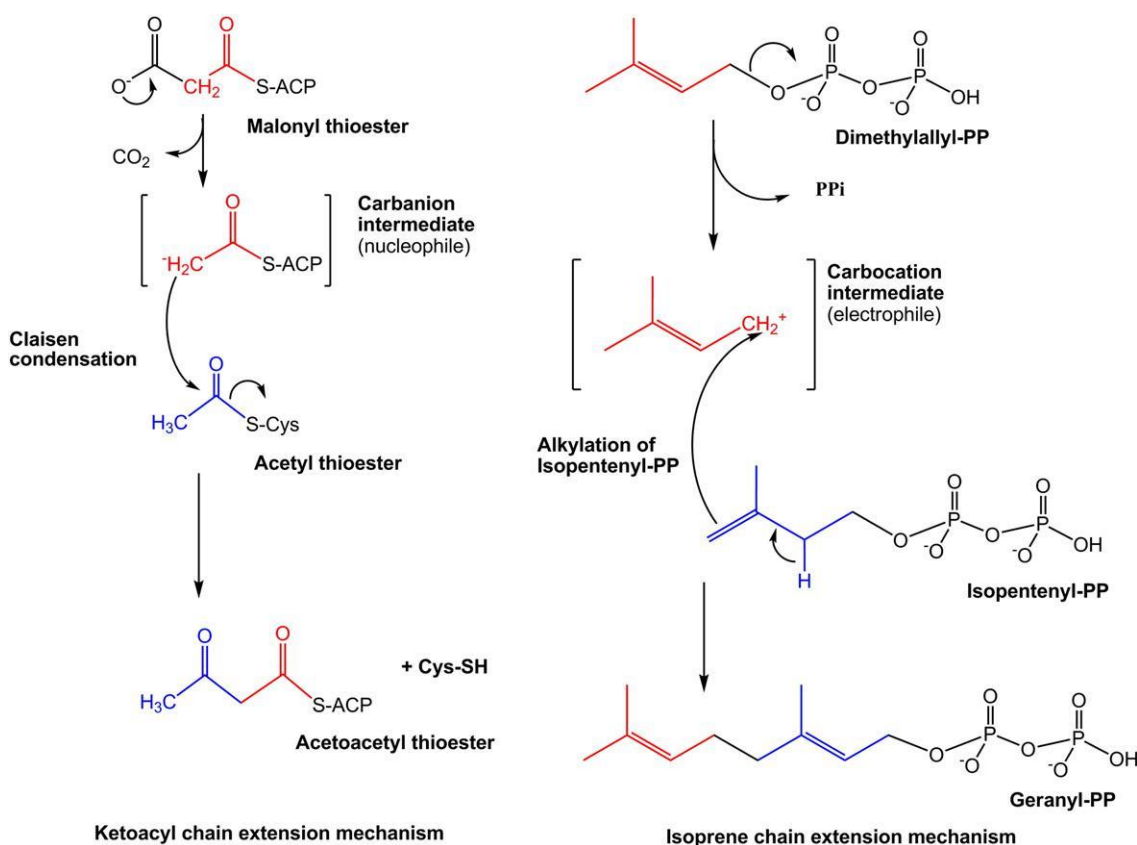


Figure 2: Lipid Biosynthesis (Fahy et al., 2011)

2.2 Fatty acyls

This major group includes fatty acids, alcohols, aldehydes, amines and esters too. These molecules are formed by the elongation of a preexisting acetyl-CoA primer to which is added a molecule of malonyl-CoA (Fig. 2). However, considering the purpose of this work we will only focus on fatty acids.

2.2.1 Fatty acids

Fatty acids are hydrocarbon derivatives, with a carboxyl group on one end.. Depending on the absence or presence of double bonds, fatty acids can be grouped in two types: saturated and unsaturated, respectively. Fatty acids have a key role in many of cell processes as they are energy sources resultant of their oxidation and membrane constituents. They are responsible by the regulation of some important aspects on cells and tissue as membrane structure and function, intracellular signaling pathways, transcription factor activity and gene expression and they are also precursors for the synthesis of bioactive lipid mediators (Calder, 2015). In fact, as constituents of membranes they are also precursors of signaling molecules as endocannabinoids, ceramides, lyso-phospholipids and diacylglycerols.

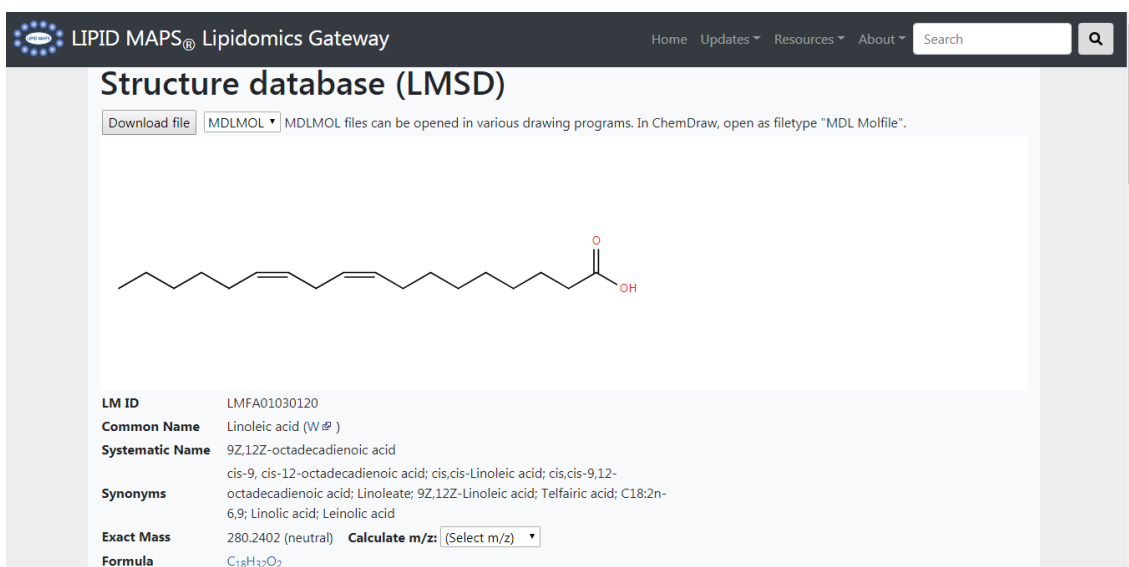
^{13}C NMR analysis of triglyceride fatty acid enrichment from ^{13}C -enriched lipogenic substrates

As part of their signaling functions, fatty acids interact with gene expression by regulating the expression or activity of transcription factors. These interactions are important in the regulation of many metabolic pathways including fat oxidation and de novo lipogenesis. Through these and other mechanisms, fatty acids play an important role in metabolic control and changes in fatty acid metabolism are associated with disease risk (Calder, 2015).

2.2.1.1 Structure and Nomenclature

Fatty acids can be identified by their LIPID ID, by their numerical identifier and finally by their familiar name. The nomenclature for the LIPID ID works as mentioned above for the general case of lipids.

On the other hand, in the numerical identifier the number on the left says respect to the number of carbons presents in the fatty acid and the number right after the colon gives us the information about how many double bonds are in the fatty acid. Finally, the numbers after the delta sign indicates the location of the double bond, taking in account that the carboxyl carbon it's the number 1 carbon, so the counting should start by the carboxyl end.



The screenshot displays the LIPID MAPS Lipidomics Gateway interface. The main heading is "Structure database (LMSD)". Below this, there is a "Download file" button and a dropdown menu for "MDLMOL" files. The chemical structure of Linoleic acid is shown as a skeletal structure with a carboxylic acid group at the end. Below the structure, the following information is provided:

LM ID	LMFA01030120
Common Name	Linoleic acid (W#)
Systematic Name	9Z,12Z-octadecadienoic acid
Synonyms	cis-9, cis-12-octadecadienoic acid; cis,cis-Linoleic acid; cis,cis-9,12-octadecadienoic acid; Linoleate; 9Z,12Z-Linoleic acid; Telfairic acid; C18:2n-6,9; Linolic acid; Leinolic acid
Exact Mass	280.2402 (neutral) <input type="text" value="Calculate m/z: (Select m/z)"/>
Formula	C ₁₈ H ₃₂ O ₂

Figure 3: Print Screen relating the nomenclature and structure of Lineolate in the LIPID MAPS database

For example, the fatty acid in Fig. 2 says respect to the lineolate (familiar name) which have the following LIPID ID: LMFA01030120.

18:Δ9,12 is the numerical identifier, and as we can confirm from the figure above it's a 18 carbon fatty acid with a double bond in the carbon 9 and 12 (counting from carboxyl group).

^{13}C NMR analysis of triglyceride fatty acid enrichment from ^{13}C -enriched lipogenic substrates

According to the absence or presence of double bonds, fatty acids can be classified as being saturated or unsaturated, respectively. For the specific case of unsaturated fatty acids with only one double bond they are named monounsaturated and the ones with two or more unsaturations are named polyunsaturated.

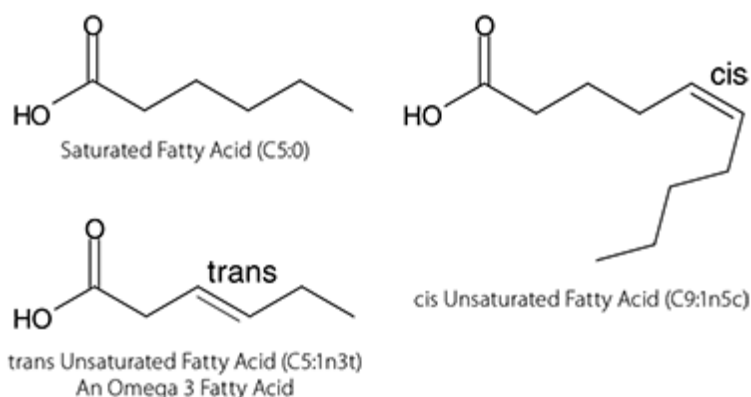


Figure 4: Structure of saturated, unsaturated, cis and trans fatty acids

In the case of unsaturated fatty acids, another classification system is used, based on the distance between the methyl carbon and the nearest carbon from a double bond, known as omega classification. For instance, for omega-3 fatty acids such as those found in fish, this means that the nearest double bond from the terminal methyl end is 3 carbons away. Essential fatty acids, which cannot be synthesized by humans or mammals and must therefore be obtained from the diet include omega-3 and omega-6 species.

Besides this classification we can also consider the other classification taking into account the stereochemistry of the hydrogen atoms according to the double bonds. (Laposata, 1995) We can classify them into cis or trans (Fig. 4) according to the form they are arranged. The cis conformation makes a bend in the fatty acid chain but trans conformation doesn't. Now it's clearly that this has consequences in the biological role of each type of fatty acid causing the trans to assume the same three-dimensional structure from a chain of a saturated fatty acid, in fact this could be the cause of some diseases due to its atherogenic properties.

^{13}C NMR analysis of triglyceride fatty acid enrichment from ^{13}C -enriched lipogenic substrates

2.2.1.2 Hepatic fatty acid Metabolism

The liver is a crossroads for whole body lipid metabolism (Figure 5). It receives free-fatty acids (FFA) from diet and from adipose tissue (AT) lipolysis, of which mesenteric adipose tissue (MAT) may play a key role since it drains directly into the portal vein. The liver can also synthesize FA from acetyl-CoA via *de novo* lipogenesis (DNL). These inflows are normally balanced by mitochondrial FFA oxidation and/or FFA esterification and export via VLDL particles. In NAFLD, there is an excess of inflow via lipogenesis or FFA import which exceeds the capacity for FA oxidation and/or export.

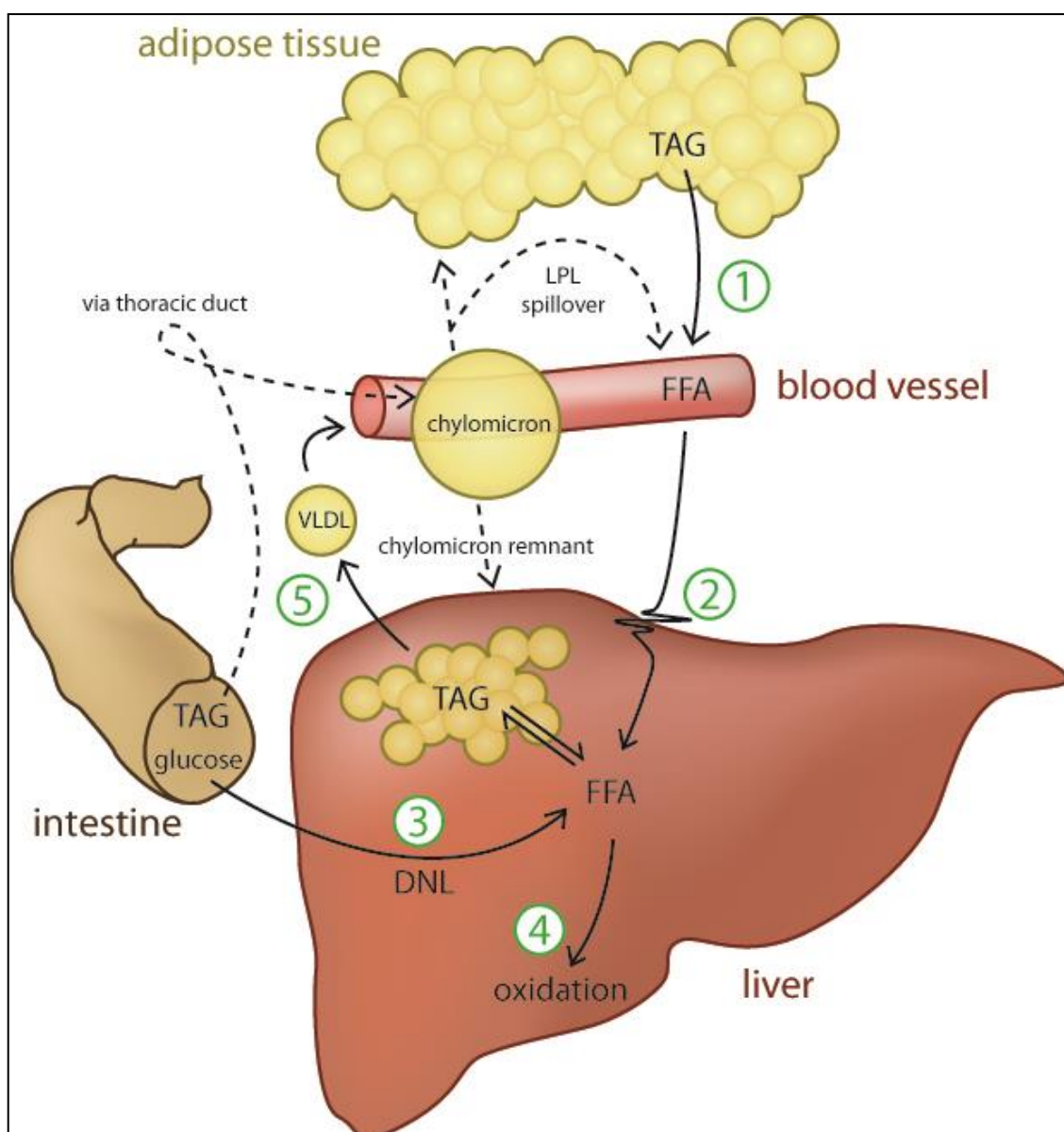


Figure 5: Hepatic fatty acid metabolism. 1-Export for the blood; 2-Import; 3-DNL; 4-Oxidation; 5-Export TAG, triacylglycerol; FFA, free fatty acids; DNL, *de novo* lipogenesis; VLDL, very low-density lipoprotein; LPL, lipoprotein lipase.

¹³C NMR analysis of triglyceride fatty acid enrichment from ¹³C-enriched lipogenic substrates

2.2.1.2.1 Fatty acid uptake

Recent findings suggests that free fatty acids freely diffuse into cells, across the plasma membrane and could be enhanced by CD36 multifunctional protein.(Xu, Jay, Brunaldi, Huang, & Hamilton, 2013) Although they mainly exist, in bloodstream complexed with albumin or in triglycerides which are themselves in the core of lipoproteins, fatty acids are available for cell uptake as free fatty acids due to the action of lipoprotein lipase present in the walls of blood vessels which hydrolysis the lipoprotein-associated triglycerides.(Chen & Farese, 2002) Once inside the cells the free fatty acids will be stored in the form of triglycerides.

2.2.1.2.2 Fatty acid Synthesis

Fatty acids production it's low in most of the cells due to the incorporation of them from the plasma, obtained from food ingestion. The biosynthetic process responsible by the production of fatty acids it's called *de novo* synthesis.

De novo fatty acids synthesis produces long chain fatty acids by the successive addition Acetyl-CoA molecules resultant from glycolysis or fructose. In the first step of this reaction the Acetyl-CoA it's carboxylated into a fragment of 3 carbons named malonyl-CoA. This step results from the direct action of acetyl-CoA carboxylase. Next, the malonyl-CoA undergoes a decarboxylative condensation with the preexisting acyl chain resulting in the increase of the acyl chain length (Sanders & Griffin, 2016).

2.2.1.2.3 Fatty acids desaturation and elongation

Once the fatty acids are synthetized or even from fatty acids obtained from the nutrition, there are some alterations that they can undergo as the insertion of double bonds or even the increase of acyl chain length.

¹³C NMR analysis of triglyceride fatty acid enrichment from ¹³C-enriched lipogenic substrates

The process by which it's inserted a new double bond in the fatty acid chains it's named desaturation and it results from the activity of several microsomal enzymes, which in fact are called desaturases. These enzymes make use of molecular oxygen and NADH to insert a desaturation at a specific position according to the type of desaturase. For example, delta-9 desaturase it's capable of insert a double bond in the middle of the ninth and tenth carbons. This kind of enzymes allow the cells to produce unsaturated fatty acids from saturated ones. Besides their activity, they are unable to change the omega type of a certain fatty acids due to their incapacity to insert a new double bond next to the last double bond and the methyl group.

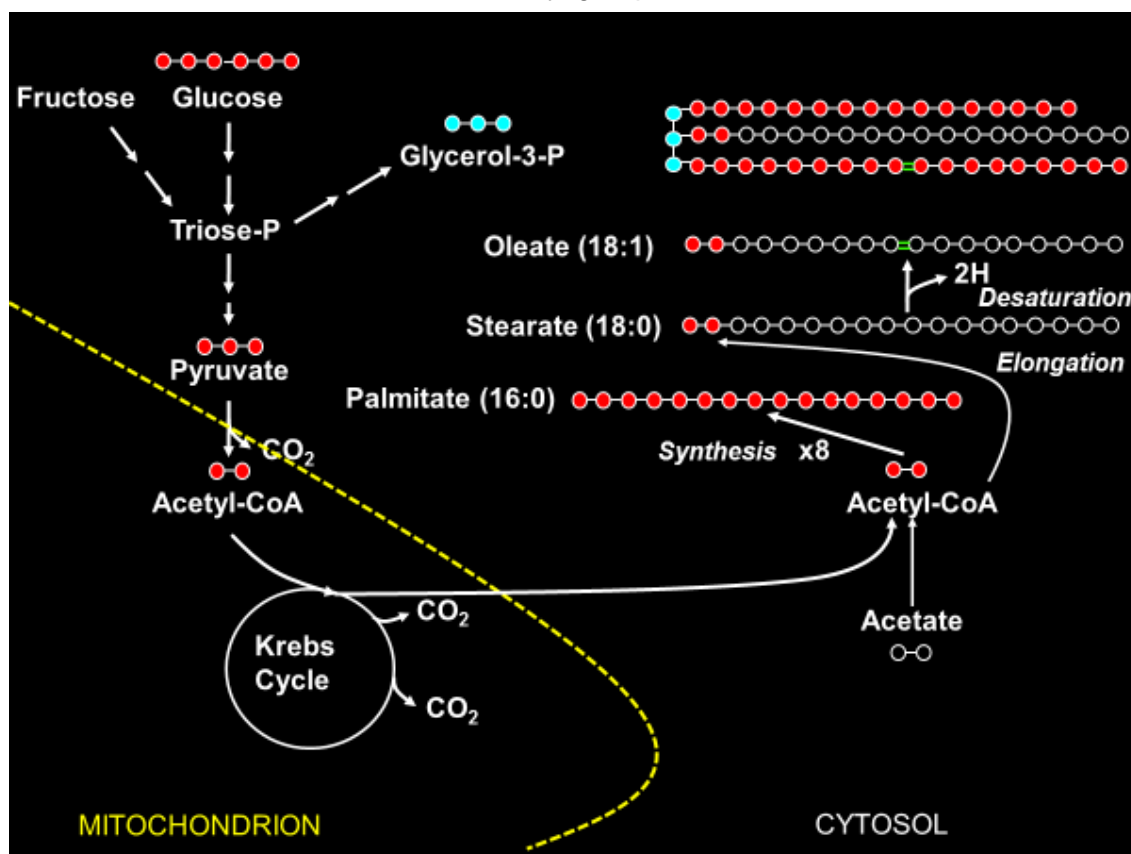


Figure 6: Fatty acid synthesis and elongation from [U-¹³C]glucose. ¹³C-atoms are represented by filled red circles and ¹²C-atoms by unfilled circles.

2.3 Glycerolipids

Glycerolipids is another class of lipids that will be one of the major focus of this work, specially the triacylglycerols (or triglycerides, which will be the term that will be used in the present work to refer to this molecules). This class includes the mono-, di and tri-substituted glycerol molecules of fatty acids. (Figure 6)

^{13}C NMR analysis of triglyceride fatty acid enrichment from ^{13}C -enriched lipogenic substrates

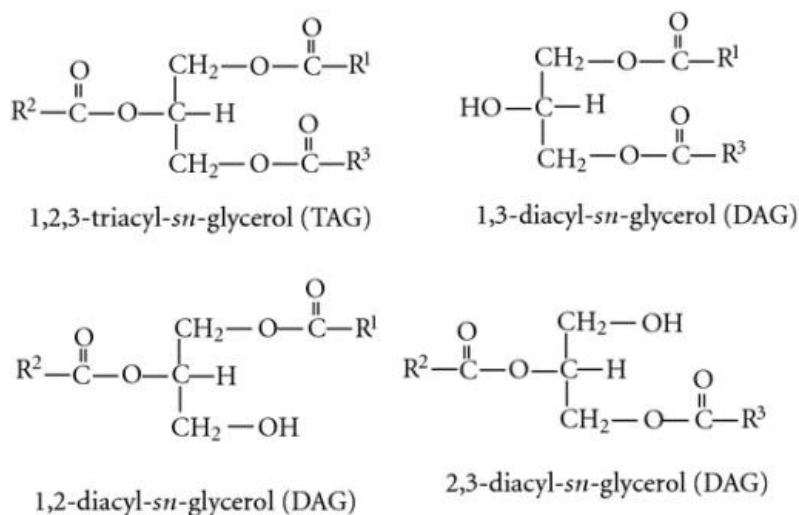


Figure 7: Mono-, di-, triacylglycerol structures

This lipids class it's in charge of energy storage in animals and plants, being present in fats or oils coming from those organisms.

According to its synthesis and the enzymes involved in that process they have an asymmetry center in the center carbon (carbon-2) of the glycerol molecule, conducting to the existence of different enantiomeric forms. This way a numbering system it's used to name these molecules, so when the stereochemistry of a glycerolipid it's known, a *sn* prefix it's used before the lipid name. The same procedure it's used for the monoacylglycerols and diacylglycerols, which normally result from the metabolism of triacylglycerols (anabolism or catabolism).

Triacylglycerols are the major contribute in terms of lipids obtained directly from diet, they can come from a variety of fats used in the human diet, from the olive oil to the fat present in the adipose tissue from fish or bovine meat. However, all these kinds of fat have in common their fatty acid profile complexity, which is related to with the numerous variations in the chain length, saturation and stereochemistry.

Nowadays there are some evidences that the fatty acid distribution among the positions 1,2 and 3 from the triglycerides it's not random. Besides that, there is an increased interest in the positional fatty acid composition of triglycerides due to the different fates of each fatty acid chain according to its position in the glycerol backbone. (Brockerhoff, Hoyle, & Wolmark, 1966; Gouk, Cheng, Ong, & Chuah, 2012) So, the focus of this work will be the analysis of the distribution from different species of fatty acids in the triglycerides.

¹³C NMR analysis of triglyceride fatty acid enrichment from ¹³C-enriched lipogenic substrates

2.3.1 Triacylglycerol Metabolism

2.3.1.1 Digestion of dietary triglycerides

The digestion of triglycerides begins with the action of lipases present in the mouth and in the stomach, this particular lipase is specific for fatty acids chain with a length from 6 to 12 carbons.

However, the bigger event in the triglycerides digestion occurs when they reach the intestine. By the action of pancreatic lipase which hydrolyzes the fatty acids esterified in the *sn*-1, 3 positions originating 2 free fatty acids and 2-monoacylglycerol. As we can see this is particular important because it results in two different fates.

The free fatty acids and the 2-monoacylglycerol are ready to permeate through the intestinal villi. As soon as these lipids pass across the membrane of intestinal epithelial cells, the 2-monoacylglycerol is esterified with 2 free fatty acids by the action of mono- and diacylglycerol acyltransferases.

So, during all this process the fatty acid in the *sn*-2 position is conserved, which just by itself is a curious aspect, but along with that it is known that dietary fats with high saturation in the *sn*-2 position are more atherogenic (Berry, 2009).

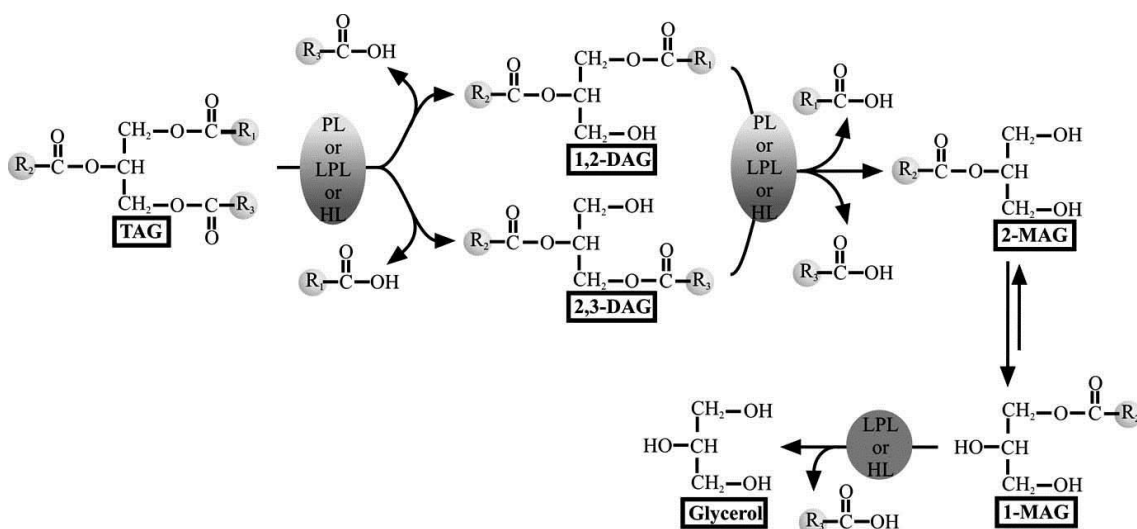


Figure 8: Triglycerides metabolism and uptake. Abbreviations: PL: Hepatic lipase; LPL: Lipoprotein lipase; HP: Hepatic lipase; MAG: Monoacylglycerol; DAG: Diacylglycerol; TAG: Triacylglycerol. (Karantonis, Nomikos, & Demopoulos, 2009)

2.3.1.2 Triglycerides synthesis

Such as fatty acids synthesis, the triglycerides synthesis takes place in the liver, which in terms is the disruption point between the anabolism and catabolism of fatty acids, which is determined by the metabolic needs of the body. Besides that, even if the body

¹³C NMR analysis of triglyceride fatty acid enrichment from ¹³C-enriched lipogenic substrates

needs fatty acids, they can undergo a pathway that will lead to the synthesis of phospholipids or eventually our object or study of this work, triglycerides.

The synthesis of triglycerides undergoes the same steps as fatty acids synthesis, but once they are completed they will be esterified with a glycerol-3-phosphate backbone, which have been obtained from dihydroxyacetone phosphate, an intermediate from glycolysis which suffered the action of glycerol-3-phosphate dehydrogenase; or from free glycerol which have been converted to glycerol-3-phosphate by glycerol kinase; and finally from pyruvate which undergoes different metabolic process which lead to the formation of dihydroxyacetone that will suffer the action of glycerol-3-phosphate dehydrogenase.

After we obtain the glycerol backbone it will be esterified with a fatty acyl-CoA at the carbon 1 of glycerol to form lysophosphatidic acid. In fact, this reaction it's catalyzed by the action of acyl-CoA:sn-glycerol-3-phosphate 1-O-acyltransferase, this enzyme could be found in mitochondrial and endoplasmic reticulum isoform. Specifically, the mitochondrial isoform it's highly specific for saturated fatty acyl-CoA which explains the high prevalence of this type of fatty acyls in the *sn-1* position of triglycerides, one more evidence that the positional fatty acid composition could play a significant role in the lipids metabolism. Besides that, the esterification of *sn-2* position it's catalyzed by acyl-CoA:1-acylglycerol-3-phosphate acyltransferase and finally the last one it's catalyzed by diacylglycerol acyltransferase arising the complete triglyceride (Karantonis et al., 2009).

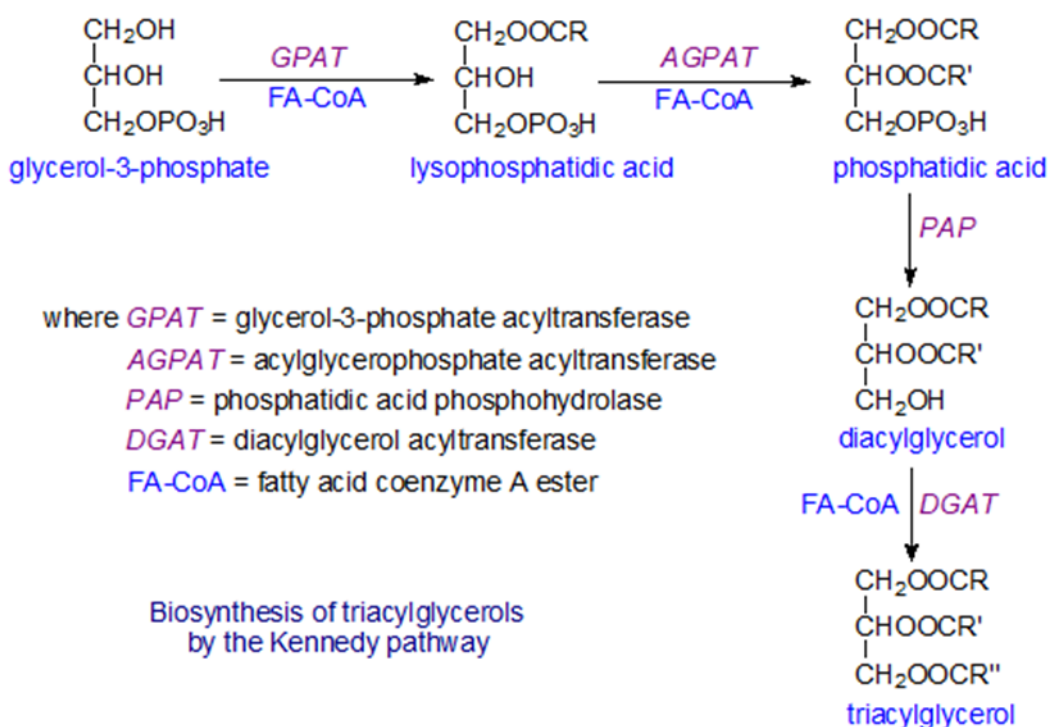


Figure 9: Main pathway of triglycerides synthesis from fatty acyl-CoA and glycerol-3-phosphate in the liver.

3 NMR analysis of lipids

3.1 Overview of NMR in molecular structure analysis

Nuclei of atoms that have either an odd mass or atomic number have a property known as nuclear spin, among them ¹H, ¹³C, ³¹P and ¹⁵N. NMR spectroscopy exploits the interaction between a particular nucleus and its surrounding chemical environment. Nuclear spins have quantum numbers (*I*) consisting of half-integers and these have $2I + 1$ possible orientations in a magnetic field. Thus, a nucleus with $I = \frac{1}{2}$ will have 2 possible orientations: aligned with the magnetic field or aligned opposite to the field. Nuclei with higher *I* values (for example 5/2 for ¹⁷O) will have more possible orientations, which among other things leads to more complex spectra and less resolved signals. For structure determination of organic molecules, nuclei with $I = \frac{1}{2}$ - which include ¹H, ¹³C and ¹⁵N - are more useful. The interactions of such nuclei with an applied magnetic field involves changes in spin states whose energy differences correspond to the radiofrequency (RF) range of the electromagnetic spectrum.

Excitation of these spin states by RF input followed by the detection of emitted RF after their relaxation to the ground state is the basis of NMR spectroscopy. Nuclear spin interactions with their immediate chemical environment include shielding by the electrons surrounding each nucleus as well as spin-spin coupling with neighboring nuclear spins. The shielding effect result in a segregation of the resonances according to the chemical environments that surrounding the nuclei in the molecule of study, while spin-spin coupling results in a well-defined signal splitting for the nuclei involved. These, as well as many other interactions, combined provide in-depth information on molecular structures. Based on this, NMR can be used to empirically identify a molecule through a unique fingerprint spectrum. In addition, the NMR signals can provide precise information about the structure and conformation of a molecule (Keeler, 2002).

Because the change in energy states of the nuclear spin is relatively low, in accordance with the Maxwell-Boltzmann distribution predictions, there exists a very small excess of nuclear spins in the ground versus excited state. For this reason, NMR spectroscopy is inherently far less sensitive compared to other spectroscopic methods that involve much greater changes in energy state (for example UV-VIS and fluorescence spectroscopy). Many advances in NMR analysis have relied on increasing the energy difference between the ground and excited states of nuclear spins, principally by designing ever more powerful magnets that expose the nuclei to higher magnetic fields. For any nucleus, the sensitivity of an NMR spectrometer is proportional to (magnetic field)^{3/2}.

¹³C NMR analysis of triglyceride fatty acid enrichment from ¹³C-enriched lipogenic substrates

Among other things, this means that an instrument with a field strength of 800 MHz has more than twice the sensitivity of a 400 MHz instrument. In addition, the signal dispersion is directly related to field strength, meaning that the absolute difference in frequency between two signals (in Hz) at 800 MHz is twice that at 400 MHz. This means that for a given sample, the NMR signals are twice as resolved at 800 MHz compared to 400 MHz allowing better characterization and quantification of crowded spectral regions. New developments in NMR probes have provided additional improvements in sensitivity. For example, cryogenic probes provide up to a fourfold improvement in sensitivity by reducing the background electronic noise (Tokunaga & Okamoto, 2010). NMR sensitivity also depends on the nucleus being observed, which is related to its gyromagnetic ratio, γ , with a higher value of γ corresponding to higher sensitivity. γ is directly related with the resonance frequency, ω_0 , of a nucleus under the action of a magnetic field with a strength of B_0 , by the following equation: $\omega_0 = \gamma B_0$ (MARTIN & CROUCH, 1991). Thus, a nucleus with higher γ resonates at a higher resonance frequency for a given magnetic field strength compared to a nucleus with a lower γ value.

Another feature that makes NMR an extremely versatile technique is the proportionality of the number of spins from a particular resonance with its signal intensity. Thus, the NMR signal intensity of a nucleus can be related to its absolute concentration. For sample analysis, an internal standard of known concentration can be added to obtain concentrations of the analyte provided that its signal does not overlap with those of the analyte. In the absence of an internal standard, the relative concentrations of different molecules can be estimated from their respective signal ratios. In the specific case of lipidomics, the NMR technique can be used to discriminate the alterations in the lipids structure and in their biological dynamics.

¹H NMR spectroscopy of lipids

Almost all organic molecules contain protons (¹H), and this nucleus has the highest γ value for a stable isotope. Thus, ¹H NMR has the highest sensitivity and application for organic molecule analysis. Its main limitation is the relatively low dispersion of ¹H signals from nuclei that have a close chemical equivalence. For lipids, this includes the protons attached to the carbon chain of fatty acids. Thus, there are few if any fully resolved signals from individual fatty acid protons, but instead there are clusters of resonances representing protons attached to saturated and unsaturated carbons of the fatty acid chain. Therefore, while ¹H signals from individual fatty acid species cannot be assigned, ¹H NMR can provide average information on triglyceride fatty acyl residues according to

¹³C NMR analysis of triglyceride fatty acid enrichment from ¹³C-enriched lipogenic substrates

their level of unsaturation and chain length. Miyake, Yokomizo, & Matsuzaki, 1998 successfully determined the unsaturated fatty acid composition in rapeseed and soybean oil by ¹H NMR. They were able to quantify the percentage of linoleic acid, linolenic acid and oleic acid by measuring the relative intensities of each fatty acyl resonance.

Barison et al., 2010 developed a new methodology which takes in account some intrinsic aspects of each fatty acyl residue which let them directly quantify each one of them from the spectra.

¹³C NMR spectroscopy of lipids

When discussing ¹³C NMR spectroscopy, it is assumed that the spectra are acquired with broadband ¹H-decoupling which eliminates ¹³C signal splitting from heteronuclear ¹³C-¹H coupling interactions. Compared to ¹H, the ¹³C nucleus has a lower γ (about $\frac{1}{4}$ that of ¹H) and its abundance in nature is only 1.1% (i.e. about 1 in every 100 carbons). Thus, the sensitivity for ¹³C observation of molecules not enriched above natural abundance is far below that of ¹H. However, this disadvantage is more than offset by the following features:

- a) Its low natural abundance simplifies ¹³C spectra due to the virtual absence of ¹³C-¹³C spin-spin coupling interactions. In probabilistic terms, the chances of having two ¹³C carbons next to each other is 0.011^2 for the first and last carbons and 2×0.011^2 for the intervening chain carbons. Thus, a ¹³C signal for a given position is composed of a singlet.
- b) the much larger chemical shift range of ¹³C (~200 ppm compared to ~10 ppm for ¹H) thereby providing increased dispersion of ¹³C signals. This is sufficient to resolve carbons of specific fatty acids in selected cases.

The lower sensitivity of ¹³C is overcome by signal averaging, which is the summing of successive free-induction decays (FIDs), resulting in an increase in the coherent signals representing the resonances relative to random noise. For dilute samples, hundreds or even thousands of FIDs need to be collected and summed hence the total collection time for ¹³C NMR spectra can extend to many hours, compared to a few minutes for ¹H NMR spectra.

Quantitative analysis of ¹³C NMR spectra needs to account for two key factors associated with the acquisition of ¹³C signals. First is the longitudinal relaxation time (T_1), which is the decay constant for the NMR signal. For rigorous quantitative analysis the NMR signal

¹³C NMR analysis of triglyceride fatty acid enrichment from ¹³C-enriched lipogenic substrates

needs to fully decay before acquisition of the next FID. Since the T_1 values of some carbons may be in the tens of seconds, the total time required to collect a large number of FIDs with sufficient delay between each FID for complete signal decay ($\geq 5 \times T_1$) may be prohibitive (Evilia, 2001). The second factor is the nuclear Overhauser effect (NOE) that accompanies ¹H decoupling. This results in a significant amplification (up to 3-fold) of ¹³C signals from carbons that are covalently bound to protons, for example the fatty acid methylene carbons, while signals from ¹³C that are not bound to protons such as the fatty acid carboxyl carbons, are unaffected. Due to constraints on the availability of spectrometer time, ¹³C NMR spectra are typically acquired with NOE and with insufficient inter-pulse interval for complete signal decay.

This results in a significant amplification (up to 3-fold) of ¹³C signals from carbons that are covalently bound to protons, for example the fatty acid methylene carbons, while signals from ¹³C that are not bound to protons such as the fatty acid carboxyl carbons, are unaffected. Due to constraints on the availability of spectrometer time, ¹³C NMR spectra are typically acquired with NOE and with insufficient inter-pulse interval for complete signal decay. Another potentially confounding effect with ¹³C NMR analysis of fatty acids is the sensitivity of the chemical shift value of some fatty acid carbons to their fractional abundance (Mannina et al., 2000). In other words, the chemical shift value of the carboxyl carbon for a specific fatty acid such as oleate is different for a triglyceride consisting of 100% oleate compared to one where oleate comprises 10% of triglyceride fatty acids (Mannina et al, 2000). The effect of fatty acid abundance on the chemical shift of a particular carbon can be much greater in comparison to structural differences (i.e. additional carbons). This means that correct assignment of a ¹³C NMR triglyceride signal to a particular fatty acid must take its relative abundance into account.

¹³C NMR analysis of triglyceride fatty acid composition of natural oils and fats, including olive oil, coconut oil, mango fat, rice bean oil and palm oil, have been previously performed (Gouk et al., 2012), (Vlahov, 1999). In these reports, the authors identified four major clusters of fatty acid resonances corresponding to the main chemical environments in the triglyceride. Importantly, they established that certain ¹³C fatty acid signals inform its location in position 2 or in positions 1 and 3 of glycerol. Gouk et al., 2012 were able to successfully determine the positional fatty acyl composition of several natural oils and fats, but they aren't able to resolve all of the individual fatty acid constituents.

In this study, we applied ¹³C NMR to study the abundance and distribution of fatty acids in hepatic triglyceride of the mouse with the aim of providing more detailed lipidomic

¹³C NMR analysis of triglyceride fatty acid enrichment from ¹³C-enriched lipogenic substrates

information on triglyceride structure. Given the potential uncertainties in assigning chemical shifts of individual fatty acids, we analyzed their ¹³C chemical shift behavior in triglyceride standards with a range of fatty acid fractional concentrations, including those mimicking the fatty acid profile of human adipose tissue triglyceride (Garaulet, Pérez-llamas, Pérez-ayala, Martínez, & Medina, 2001). In addition, we also measured ¹³C-¹³C-coupling constants of selected fatty acid signals as a prelude to predicting the positions of ¹³C-¹³C-coupled signals from the incorporation of [U-¹³C]substrates into hepatic fatty acids via *de novo* lipogenesis.

4 Materials and Methods

4.1 Reagents and Materials

All the synthetic fatty acids methyl esters (FAME) were obtained from Sigma-Aldrich Company which were respectively methyl palmitate [$\text{CH}_3(\text{CH}_2)_{14}\text{CO}_2\text{CH}_3$; n-Hexadecanoic acid methyl ester] ; methyl oleate [$\text{CH}_3(\text{CH}_2)_7\text{CH}=\text{CH}(\text{CH}_2)_7\text{CO}_2\text{CH}_3$; Methyl cis-9-octadecenoate] and finally methyl linoleate [$\text{CH}_3(\text{CH}_2)_3(\text{CH}_2\text{CH}=\text{CH})_2(\text{CH}_2)_7\text{CO}_2\text{CH}_3$; Methyl cis,cis-9,12-octadecadienoate], all of them were have a purity $\geq 99\%$ according to the manufacturer. They were used without further purification.

Along with the FAMEs the homotriglycerides standards of glyceryl tripalmitate (T5888), glyceryl tristearate (T5016), glyceryl tripalmitoleate (T2630) and glyceryl trilinoleate (T9517) were also obtained from Sigma-Aldrich. All of them were used without any additional purification. Finally, glyceryl trioleate (368120010) was obtained from ACROS Organics.

Isotope-labeled triglycerides were obtained from Cambridge Isotope Laboratories, Inc. The labeled triglycerides used were tripalmitin, trispalmitoyl-D93 and glyceryl-D5, which are respectively substituted in the fatty acyl chains and in the glycerol backbone hydrogen atoms.

Table 1: Standard triglyceride mixture composition

<i>Stock solutions</i>	<i>Expected ratio (mol)</i>	<i>Final ratio (mol%)</i>
<i>Palmitate</i>	18,1	16,87
<i>Palmitate-D93</i>	1,1	1,13
<i>Palmitate-glyceryl D5</i>	2,1	2,00
<i>Stearate</i>	4,3	4,31
<i>Oleate</i>	51,1	52,54
<i>Palmitoleate</i>	4,3	3,99
<i>Linoleate</i>	19,1	19,16

¹³C NMR analysis of triglyceride fatty acid enrichment from ¹³C-enriched lipogenic substrates

4.2 Standard Preparation

In first approach 3 synthetic mixtures of FAMES in equal parts were prepared. One mixture containing methyl palmitate and methyl oleate, another mix containing methyl linoleate and methyl oleate and finally the last one containing methyl palmitate and methyl linoleate. All the solutions were prepared by mixing 100 μ L of each component from a previous solution of 1 mg/mL concentration.

Besides those 3 standards another one was made including glyceryl tripalmitate, tristearate, trioleate, tripalmitoleate and trilinoleate. The proportions of these fatty acids in the mixture was matched to that measured in human adipose tissue triglyceride and they account for 94% of the total fatty acid content (Garaulet et al., 2001). For modelling deuterium labeling studies (not the focus of this Thesis work) a small percentage of the glyceryl tripalmitate was enriched with deuterium in the fatty acid chains (D93) as well as the glyceryl moiety (D5). Thus, the mixture was composed of 10,94 mg of glyceryl tripalmitate; 0,73 mg of glyceryl tripalmitate-D93; 1,30 mg of glyceryl tripalmitate-D5; 2,80 mg of glyceryl tristearate; 34,09 mg of glyceryl trioleate; 2,59 mg of glyceryl tripalmitoleate and 12,43 mg of glyceryl trilinoleate. Table 1: Standard triglyceride mixture composition .

4.3 Thin Layer Chromatography

To confirm the presence of triglycerides or methyl fatty acyl species, thin layer chromatography was performed. The eluent used was a mixture of petroleum ether/diethyl ether/acetic acid in a proportion of 7:1:0,1 respectively. The plate used were obtained from Sigma-Aldrich company. When the eluent reached 2 cm from the top of the plate the plate was allowed to dry and then was stained with iodine vapor.

4.4 Biological Samples

The biological sample were obtained from 12-week-old C57BL6 mice. The mice were feed with standard chow. The animals were euthanized and the liver and the fat tissues were rapidly extracted and rapidly frozen using liquid nitrogen then they were stored until further being processed.

The following step was the triglycerides extraction through the usage of solid-phase extraction columns obtained from Sigma-Aldrich Company (52657-U). First the column was washed with 8 mL of hexane and 24 mL of hexane/methyl tert-butyl ether and then the tissues were prepared by dissolving them in 800 μ L of hexane/methyl tert-butyl ether (96:4) and then load on the column. Then the column was eluted with 32 mL of

¹³C NMR analysis of triglyceride fatty acid enrichment from ¹³C-enriched lipogenic substrates

hexane/methyl tert-butyl ether and 4 mL fractions were collected. To finish the fractions were subjected to TLC analysis to confirm the presence of triglycerides. The fractions with triglycerides will be mixed together and then evaporated to further analysis (Hamilton & Comai, 1988).

4.5 NMR spectroscopy

All ¹H and ¹³C NMR spectra were obtained using a Varian VNMRS 600 MHz NMR (Agilent, Santa Clara, CA, USA) spectrometer equipped with a 3 mm broadband probe with z-gradient. ¹³C NMR spectra were obtained at a temperature of 25°C, using a sweep width of 30 KHz, 70° pulse, 2.5 seconds acquisition time and 0.5 second pulse delay. For each spectrum, 1,000-15,000 FID were obtained corresponding to ~1-15 hours of collection time per spectrum. Fully relaxed ¹H NMR spectra of TAG samples were obtained were acquired with a sweep width of 8 KHz, a 90° pulse and 8 s of recycling time (3 s of acquisition time and 5 s pulse delay). A total of 16 FIDs were acquired for each ¹H NMR spectrum.

Spectra were analyzed with ACD/NMR Processor Academic Edition software (ACD/Labs, Advanced Chemistry Development, Inc.).

5 Results and Discussion

5.1 NMR Assignments

5.1.1 ¹³C NMR

In the past few years, several works have assigned the constituent carbon atoms from triglycerides. Furthermore, four major clusters of resonances are described in literature (Vlahov, 1999) (Figure 10):

- Methylenic region from 10 to 35 ppm which correspond to the resonances of methyl and methylene carbons from the fatty acyl chains, (saturated and unsaturated);
- Glycerol region from 60 to 72 ppm which correspond to the resonances from the glycerol backbone carbons;
- Olefinic region, from 124 to 134 ppm, which corresponds to the unsaturated carbon resonances;
- Carbonyl region, from 172 to 174 ppm, which corresponds to the carbonyl carbons from the fatty acyl chains.

In the present work the main focus will be the methylenic region in addition to the carbonyl region, which in fact was already studied in detail by Gouk et al., 2012.

Because of the marked concentration dependence of the chemical shifts on the fatty acyl concentrations (Mannina et al., 2000), during this section, the assignments will be based in the comparison between the different fatty acyls species and their structure.

^{13}C NMR analysis of triglyceride fatty acid enrichment from ^{13}C -enriched lipogenic substrates

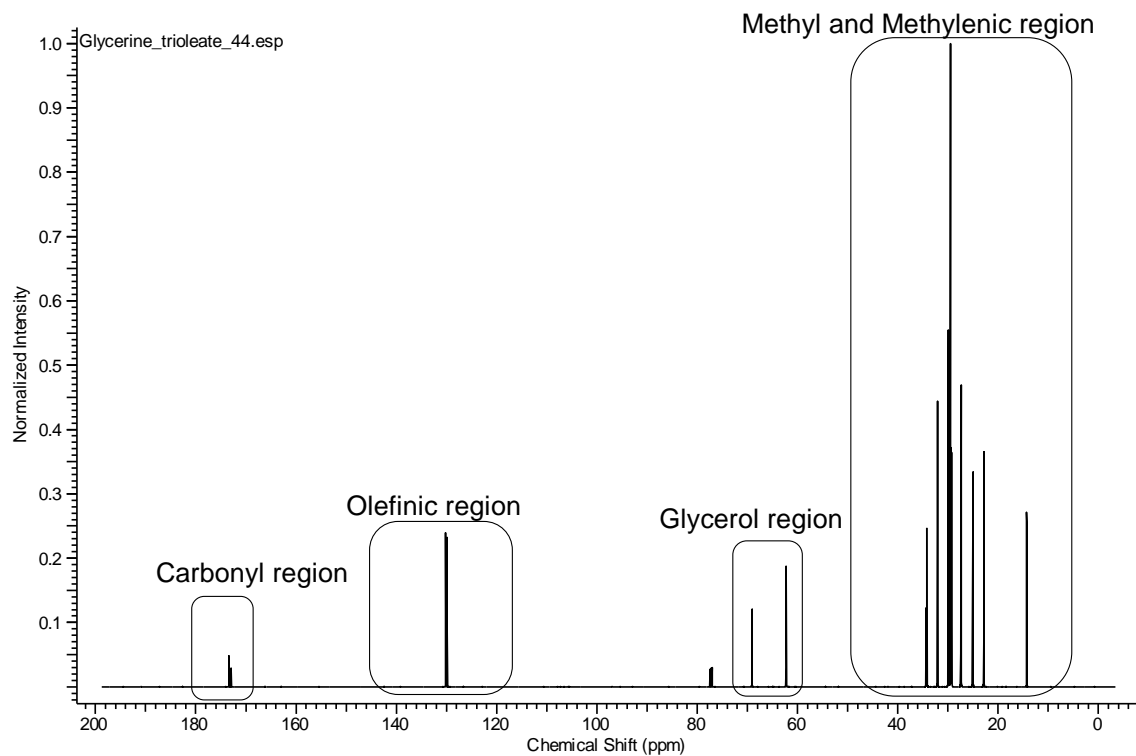


Figure 10: 600 MHz ^{13}C NMR spectrum of glyceryl trioleate, with the respective clusters from the Carbonyl, Olefinic, Glycerol and Methyl and Methylenic carbons resonances.

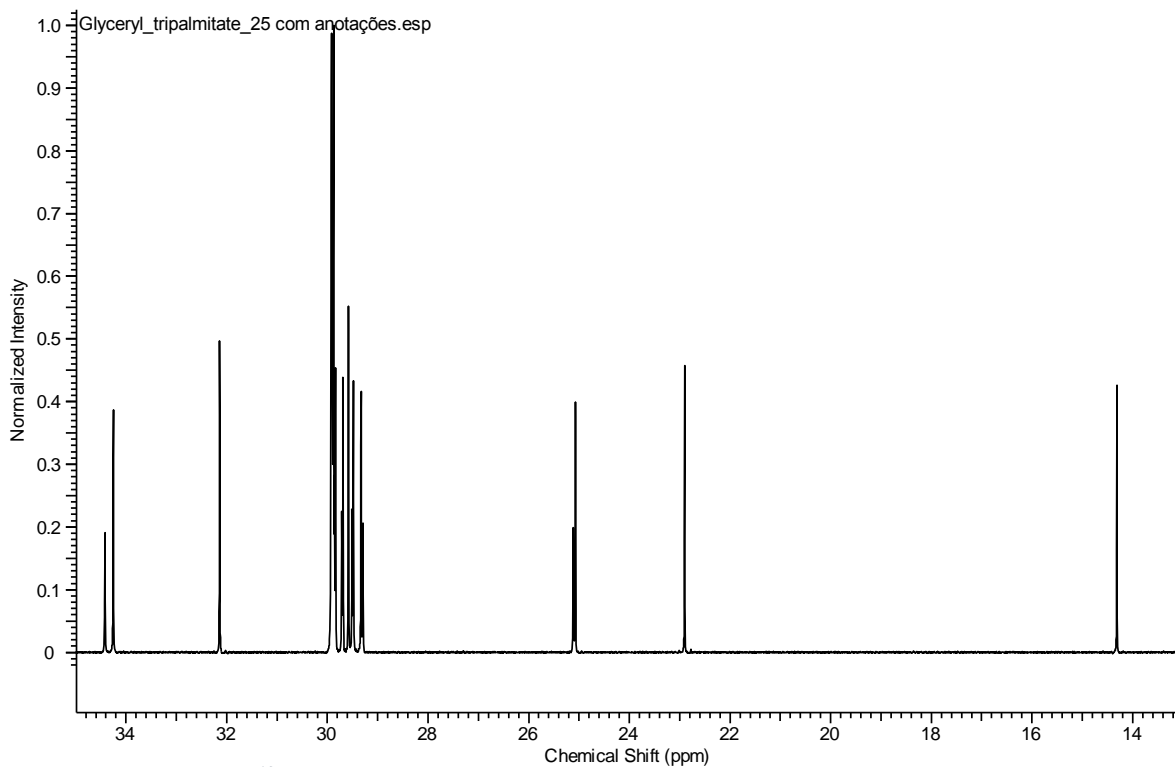


Figure 11: 600 MHz ^{13}C NMR spectrum of a glyceryl tripalmitate standard.

^{13}C NMR analysis of triglyceride fatty acid enrichment from ^{13}C -enriched lipogenic substrates

The first cluster, which corresponds to the resonances from 14 to 35 ppm (see Figure 11) and says respect to the carbons from the fatty acyl chains.

The 14 ppm peak corresponds to the terminal carbon from the fatty acyl chain (see Figure 12), according to Vlahov, 1999. The chemical shift of this signal shows small variations depending on the nature of the fatty acyl. For the fatty acids studied, the chemical shift signal seems to be the least sensitive to changes in fatty acid concentration.

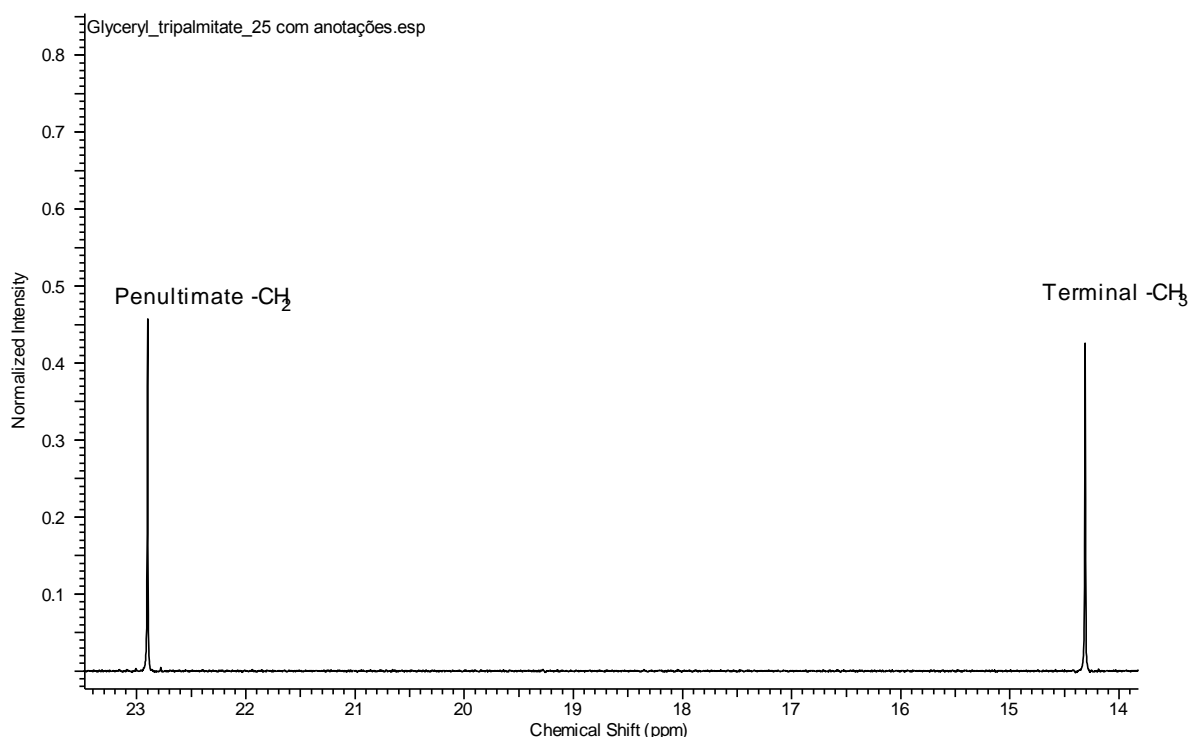


Figure 12: Methyl and methylenic carbon region of 600 MHz ^{13}C NMR spectrum of glyceryl tripalmitate.

As we move left in the spectrum we find another set of peaks in the 22 ppm region (see Figure 11) which correspond to the resonance of the penultimate carbons from the fatty acyl chains once more this assignment it's made based on the reports from literature (Vlahov, 1999).

Finally, the most upfield set of peaks from this cluster, resonating at about 34 ppm are the resonances of the fatty acids carbon 2. In this set of signals, there is clear separation between the two fatty acids occupying positions 1,3 of the glycerol backbone and the third fatty acid located on glycerol position 2. The position 2 carbons resonate at higher frequency compared to the signal from carbons 1 and 3. In accordance with the fatty acid distributions, the ratio of the signal intensities of the 1-,3- positions relative to that of position 2, is 2:1 (See Figure 13).

The cluster of signals representing the fatty acid carbonyls is also the focus of the present work. These signals are also sensitive to the fatty acid position in the glyceryl chain as for the C-2 carbons. For the carboxyl signals, those of positions 1 and 3 resonate at 0,42

^{13}C NMR analysis of triglyceride fatty acid enrichment from ^{13}C -enriched lipogenic substrates

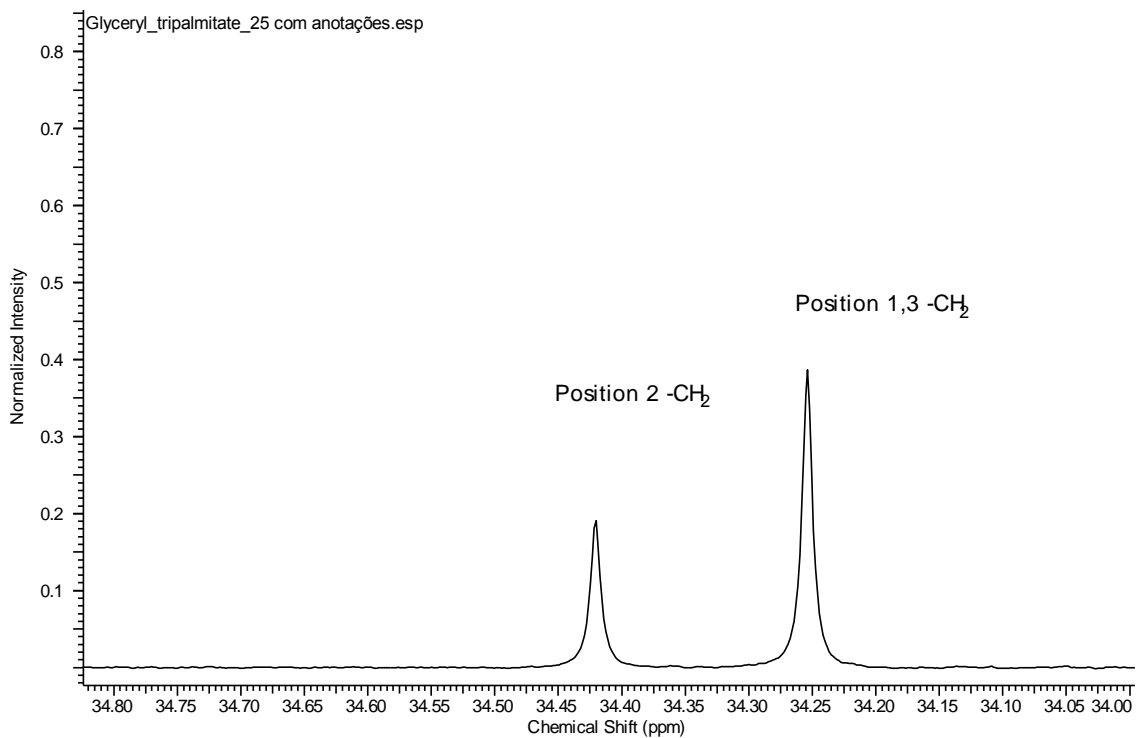


Figure 13: The C_2 region of 600 MHz ^{13}C spectrum of glyceryl tripalmitate.

ppm upfield of the signals from position 2 (Figure 14), this result from the two γ -gauche interactions on the carbonyl carbons from position 2 against just one for the carbonyl carbons in the positions 1 and 3 (Vlahov, 1999).

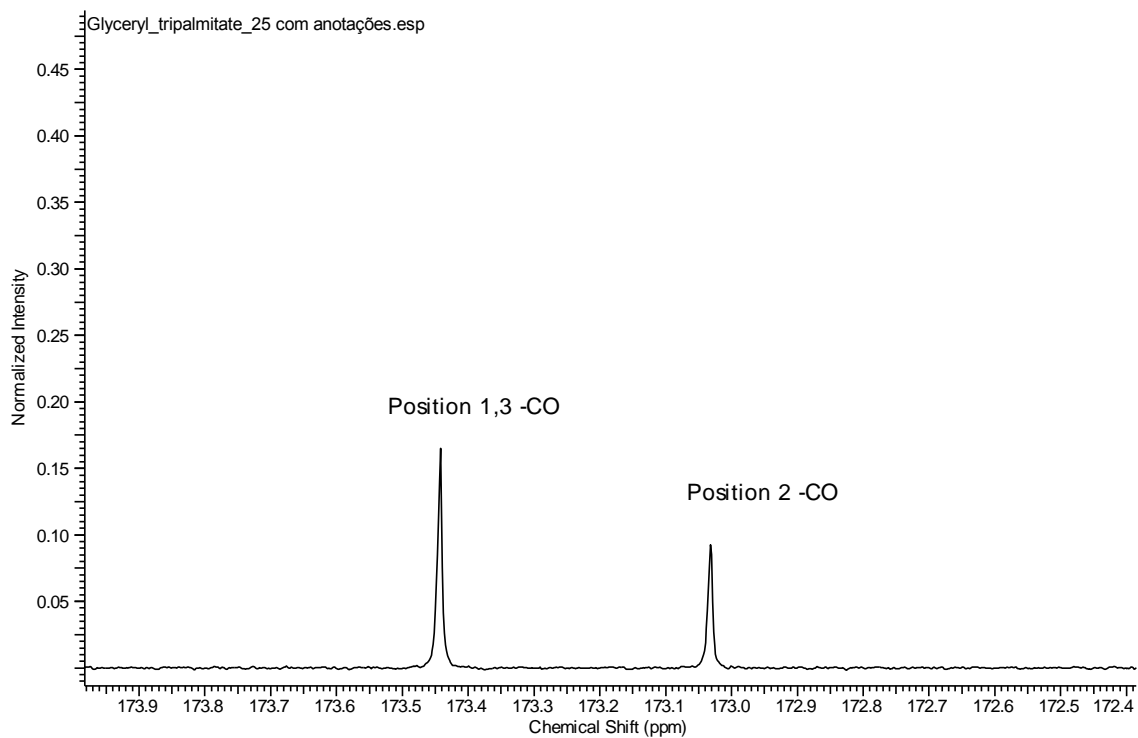


Figure 14: The carbonyl region of 600 MHz ^{13}C spectrum of glyceryl tripalmitate.

¹³C NMR analysis of triglyceride fatty acid enrichment from ¹³C-enriched lipogenic substrates

Considering the purpose of using ¹³C NMR spectroscopy as a quantitative technique the spectra need to be acquired in the same conditions, in such a way that the integration of the areas under each carbon signal could be directly proportional to the concentrations of that atom and the relation of proportionality remains constant. Therefore, if this was true, then resolved signals from individual carbons of the same fatty acid should have the same intensity. Moreover, if this was the case, then the relative abundance of two (or more) fatty acids could be precisely estimated from the ratio of any carbon signal of fatty acid 1 with any carbon signal of fatty acid 2.

However, as shown in Table 2, the signal intensities of individual fatty acid carbons carbons show large variations.

The reason for this is due to the carbons having different longitudinal relaxation times (T_1), as well as NOE effects.

Table 2: Integration areas of standard triglycerides 600 MHz ¹³C NMR spectra obtained with ACDLabs software.

Normalized area of integration/ Triglyceride specie	Terminal carbon region (14 ppm)	Penultimate carbon region (22 ppm)	C2 carbon region (34 ppm)	Carbonyl carbon region (174 ppm)
Glyceryl tripalmitate	8059732	8808353	14441917	4938074
Glyceryl trioleate	327000256	355449664	601649872	213341688
Glyceryl tristearate	774824,88	818510,5	1377265	418959,48
Glyceryl trilinoleate	11307468	11923778	24507995	7200551
Glyceryl tripalmitoleate	2474426,25	2457796,75	2611052	1201271,75
Mean Ratios	1,73	1,82	2,92	1,00

From the table, it can be seen that the carbonyl carbons have notably lower signal intensities compared to the other resonances. This is because these carbons have no directly attached protons, and therefore do not experience NOE. Also, they have long T_1 values, which leads to signal saturation under the conditions of the NMR acquisition. and higher at the C2 methylene carbon and very similar in the terminal and penultimate carbons from the fatty acyl chains. In theory, these differences in signal intensities can be minimized by using very long interpulse delays to ensure full relaxation of long T_1 nuclei and inverse gated decoupling to avoid NOE buildup. However, this would lead to

¹³C NMR analysis of triglyceride fatty acid enrichment from ¹³C-enriched lipogenic substrates

a prohibitively long collection time (many days!) for each spectrum. Therefore, under the standard acquisition conditions used for these samples, a carboxyl signal from one fatty acid cannot be directly measured against the methyl signal of another in order to obtain their relative abundance. However, since T_1 and NOE effects are very similar if not identical for equivalent carbon positions of different fatty acids, then comparing the methyl signal of one fatty acid versus the methyl signal of another can provide a precise measure of their relative abundance.

^{13}C NMR analysis of triglyceride fatty acid enrichment from ^{13}C -enriched lipogenic substrates

5.2 Standard mixture quantitative analysis

Considering the main focus of this work and all the assignments and results obtained so far, we proceeded to the quantitative analysis of the mixture presented in Table 1. The resultant spectrum it's presented in Figure 15, and in more detail in the Figure 16, 17, 18 and 19. We started by assigning each peak, taking in account the prior literature and the aforementioned assumptions from our results and the synthetic mixture ratios.

This way, the first set of peaks in the Figure 16 we can distinguish 2 resonances in the 14 ppm region which says respect to the terminal carbons from the acyl chains.

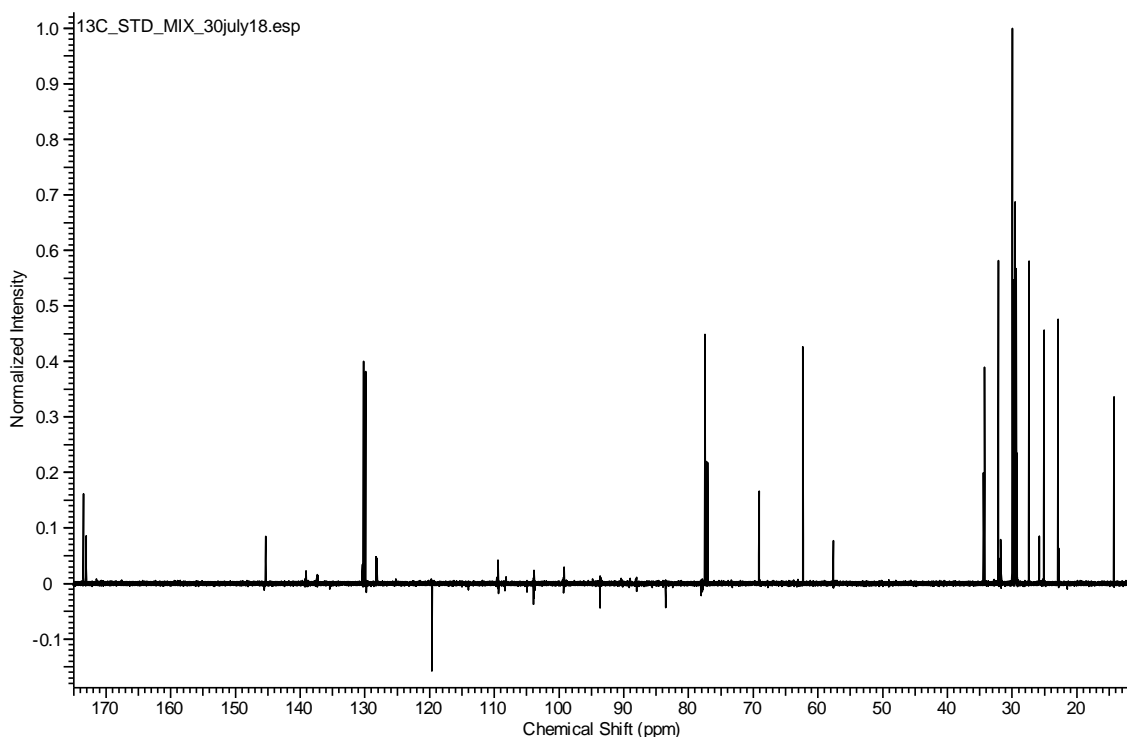


Figure 15: 600 MHz ^{13}C NMR spectra from the synthetic mixture of triglycerides.

^{13}C NMR analysis of triglyceride fatty acid enrichment from ^{13}C -enriched lipogenic substrates

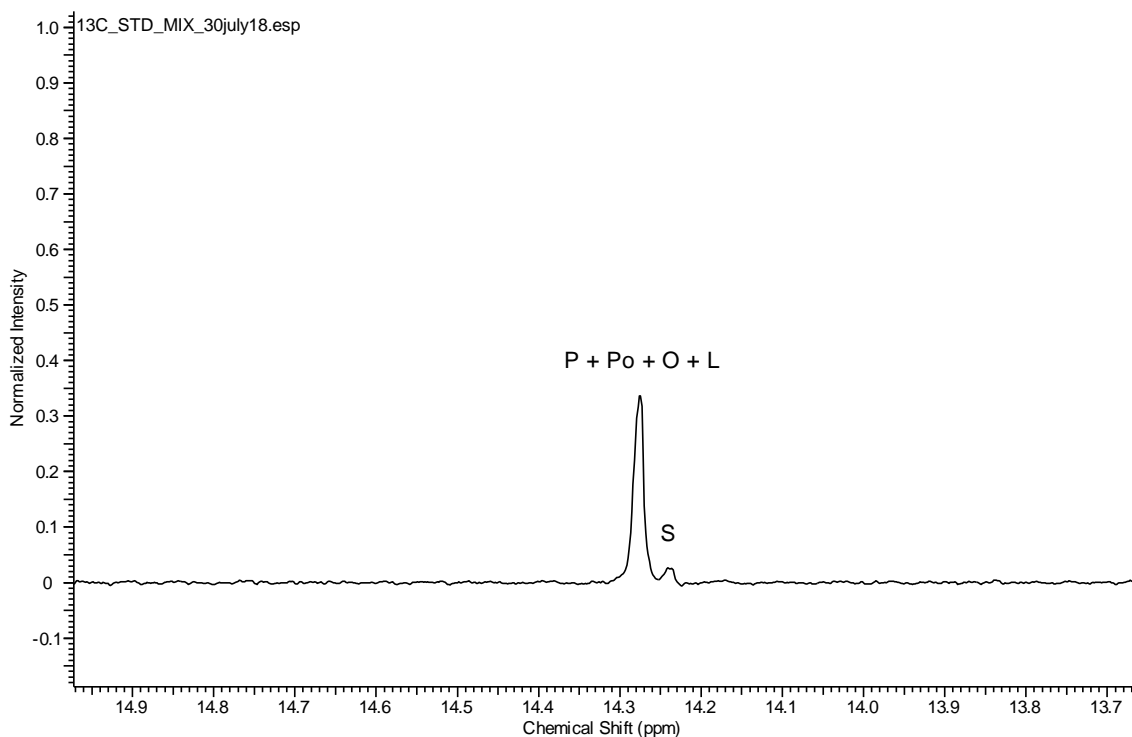


Figure 16: Terminal carbon region of 600 MHz ^{13}C NMR spectra from the synthetic mixture of triglycerides. S-stearate acyl chain; P-palmitate acyl chain; O-oleate acyl chain; Po-palmitoleate acyl chain; L-linoleate acyl chain.

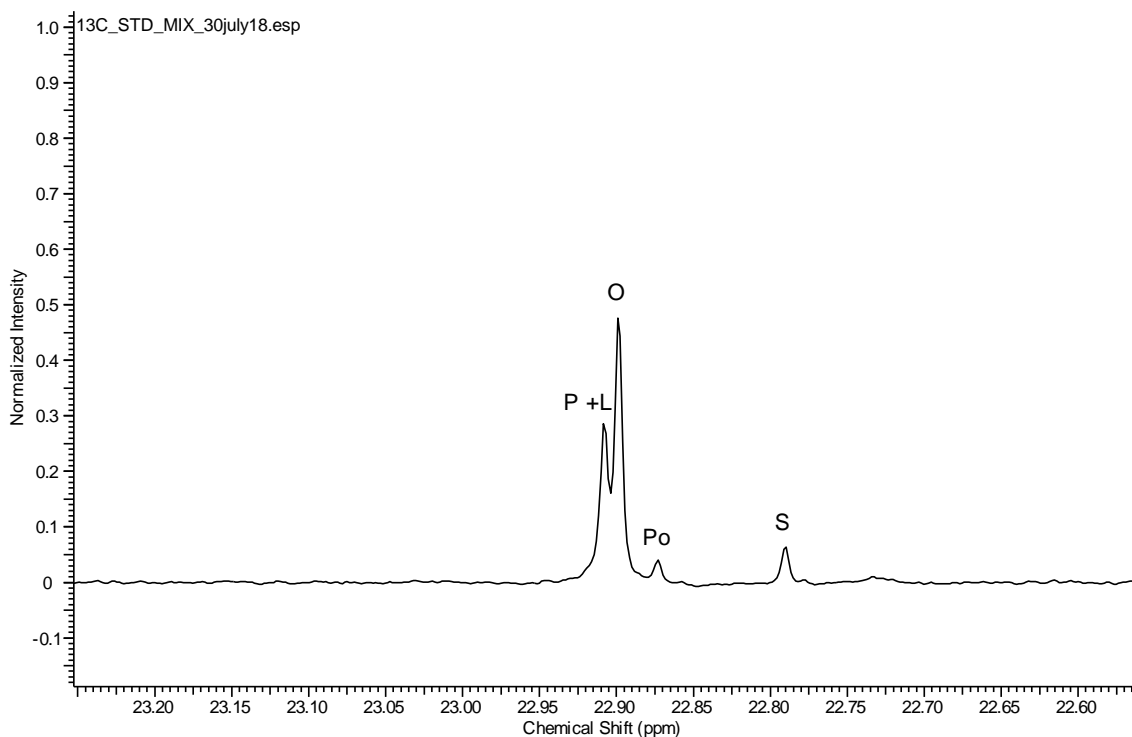


Figure 17: Penultimate carbon region of 600 MHz ^{13}C NMR spectra from the synthetic mixture of triglycerides. S-stearate acyl chain; P-palmitate acyl chain; O-oleate acyl chain; Po-palmitoleate acyl chain; L-linoleate acyl chain.

^{13}C NMR analysis of triglyceride fatty acid enrichment from ^{13}C -enriched lipogenic substrates

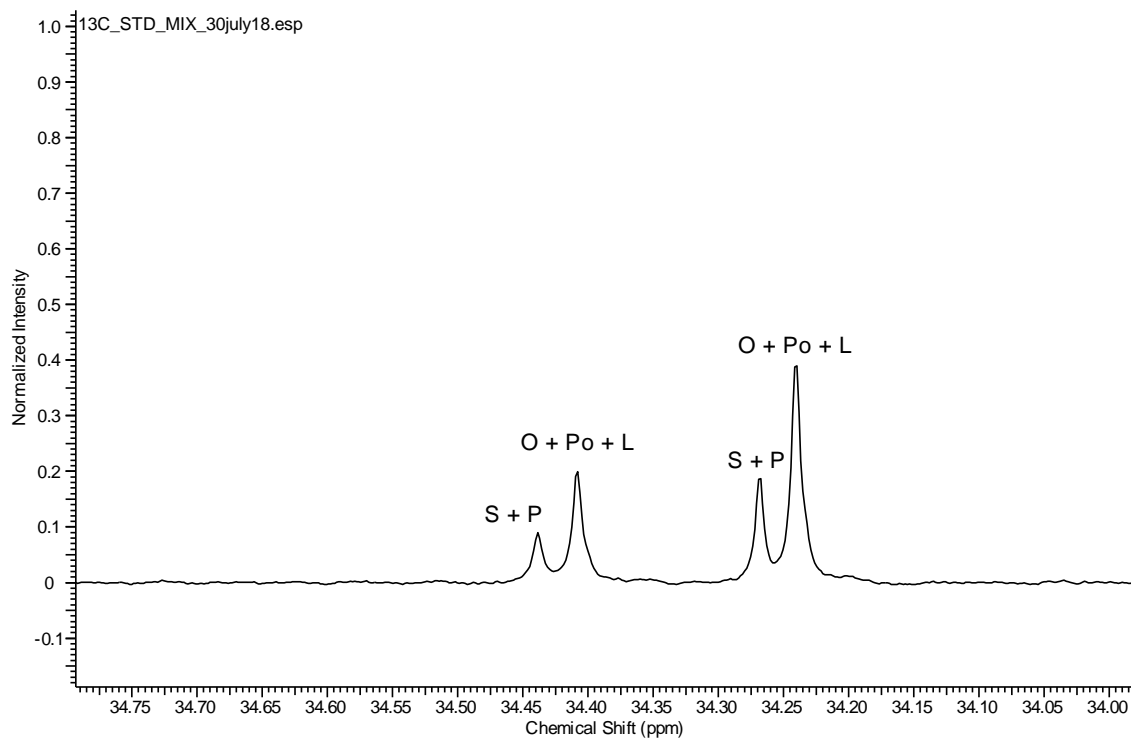


Figure 18: C_2 methyl carbon region of 600 MHz ^{13}C NMR spectra from the synthetic mixture of triglycerides. S-stearate acyl chain; P-palmitate acyl chain; O-oleate acyl chain; Po-palmitoleate acyl chain; L-linoleate acyl chain.

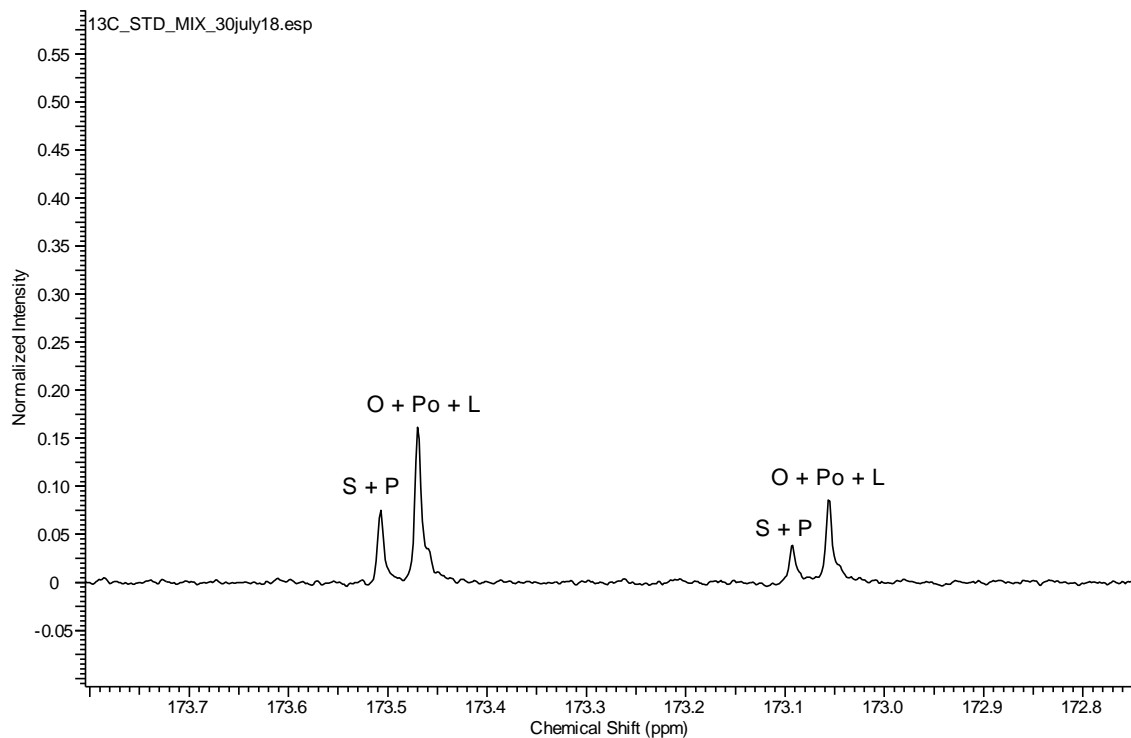


Figure 19: Carbonyl carbon region of 600 MHz ^{13}C NMR spectra from the synthetic mixture of triglycerides. S-stearate acyl chain; P-palmitate acyl chain; O-oleate acyl chain; Po-palmitoleate acyl chain; L-linoleate acyl chain.

¹³C NMR analysis of triglyceride fatty acid enrichment from ¹³C-enriched lipogenic substrates

After the integration of the total area of these signals the relative area of the two peaks was 5,18% and 94,82% (Table 3). According to the calculated composition of the mixture (Table 1) we can expect that the smaller signal corresponds to the resonance of stearate or palmitoleate fatty acyl chains.

As we pass to the penultimate carbon region (Figure 17) we obtain a ratio of 6,46%, 3,11%, 52,47% and 37,89%. So in this set of peaks we can do some significant assignments, starting for the major constituent, which will correspond to the resonance of oleate (22,9 ppm), in other and the only way to achieve a ratio of 37,89% it's if that peak correspond to the resonance of palmitate and linoleate which will give arise to a ratio of 39,15 according to the Table 1. By comparison between the ratios of stearate and palmitate and based on the bigger ratio should correspond to stearate and the minor to palmitoleate.

In the 34 ppm region we have the 4 signals which correspond to the signals from the 2-position (upfield) and from 1,3 positions (downfield). The ratios obtained were 47,80%, 17,76%, 24,57% and 9,87% taking in account the unsaturation level and the prior literature (Gouk et al., 2012) and the similar behavior to the carbonyl carbon, the signals with higher frequency correspond to the saturated fatty acyl chains and the remains to the other species. The same argument applies to the carbonyl region.

The results are summarized in Table 3 and the in more detail in Annex I.

Table 3: Relative integration areas obtained with ACDLabs from the 600 MHz ¹³C NMR spectra of the triglyceride synthetic mixture

Region (relative integration area %)			34 ppm		173 ppm		Composition (mol%)		Expecte d ratio (mol %)
	14ppm	22 ppm	Position 1,3 from glycerol backbone	Position 2 from glycerol backbone	Position 1,3 from glycerol backbone	Position 2 from glycerol backbone	Position 1,3 from glycerol backbone	Position 2 from glycerol backbone	
Stearate	5,18	6,46	17,76	9,87	17,76	10,9	5,82 *		4,31
Palmitate	94,82	37,89					21,46**		20
Oleate		52,47	52,47		52,54				
Palmitoleate		3,11	47,80	24,57	47,80	25,47	3,11		3,99
Linoleate		37,89	17,15***		19,16				
Total	100	100	66,71	33,29	66,11	33,89	100,01		100

*obtained by calculating the average between the values obtained for stearate contribution.

**obtained by subtracting the average value of stearate to the value of stearate+palmitate peaks in the 34ppm and 174 ppm region.

***obtained by subtracting the contribution of oleate and palmitoleate to the average value of the peak from oleate+linoleate+palmitoleate.

^{13}C NMR analysis of triglyceride fatty acid enrichment from ^{13}C -enriched lipogenic substrates

As we can observe, the fatty acid composition determined from ^{13}C NMR analysis of their common carbon positions was in close agreement with the expected composition of the triglyceride mixture.

^{13}C NMR analysis of triglyceride fatty acid enrichment from ^{13}C -enriched lipogenic substrates

5.3 Biological samples

Following the methodology mentioned above, the next step will be applying it biological samples. ^{13}C NMR spectra from visceral fat of 12-week-old mice were obtained and the resultant spectra is shown in Figure 20.

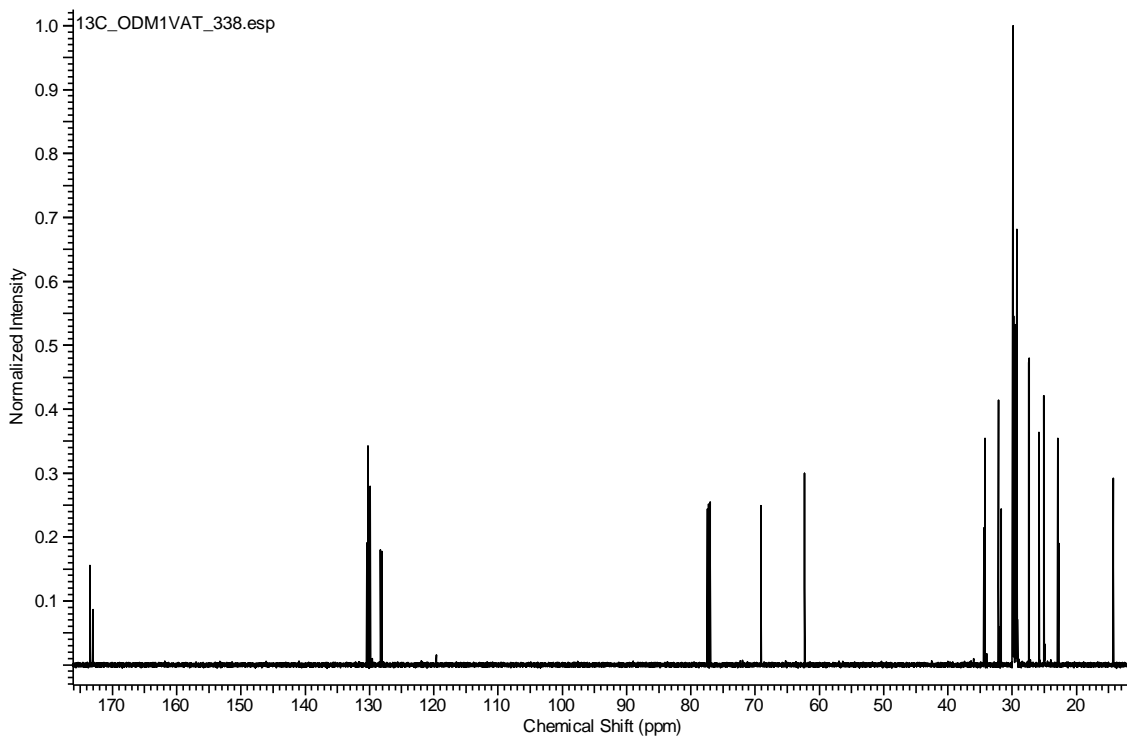


Figure 20: 600 MHz ^{13}C NMR spectra of visceral fat from 12-week-old mouse.

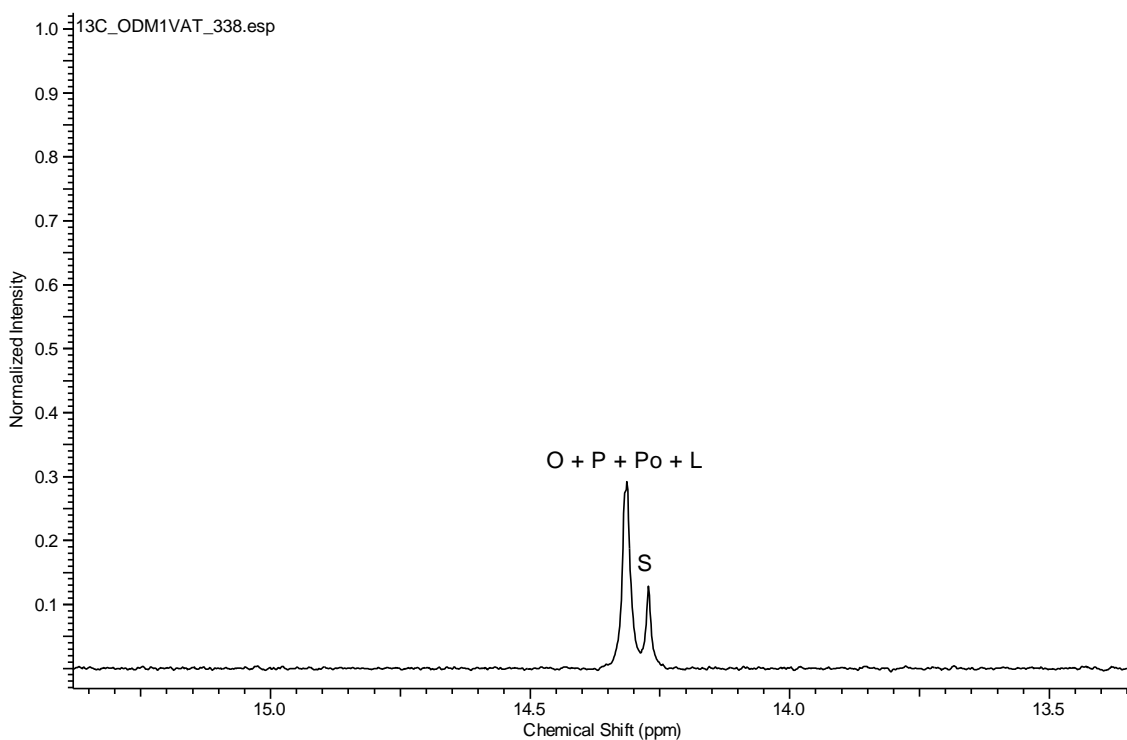


Figure 21: Methyl carbon region of 600 MHz ^{13}C NMR spectra of mouse visceral fat from a 12-week-old mouse. S-stearate acyl chain; P-palmitate acyl chain; O-oleate acyl chain; Po-palmitoleate acyl chain; L-linoleate acyl chain.

^{13}C NMR analysis of triglyceride fatty acid enrichment from ^{13}C -enriched lipogenic substrates

Taking in account the assignments established above for the 14 ppm region we will have the C_{18} of stearate in the lower frequency and the remaining ones on the higher frequency peak. See Figure 21.

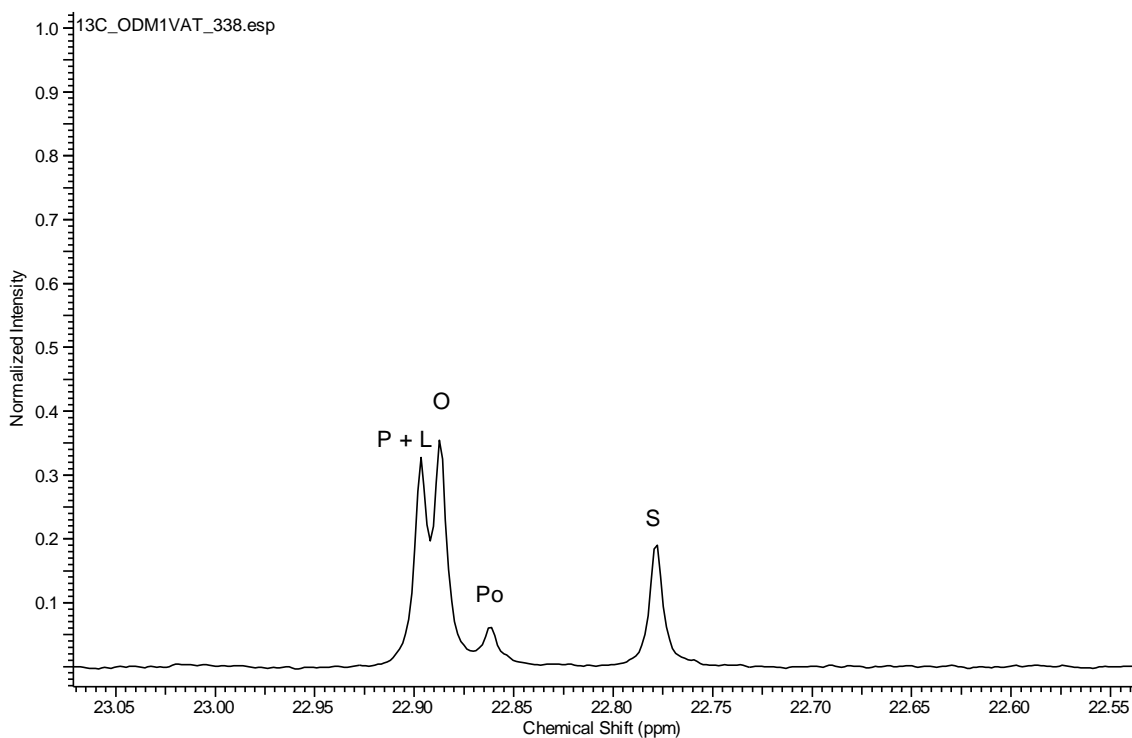


Figure 22: Penultimate carbon region of 600 MHz ^{13}C NMR spectra of mouse visceral fat from a 12-week-old mouse *S*-stearate acyl chain; *P*-palmitate acyl chain; *O*-oleate acyl chain; *Po*-palmitoleate acyl chain; *L*-linoleate acyl chain.

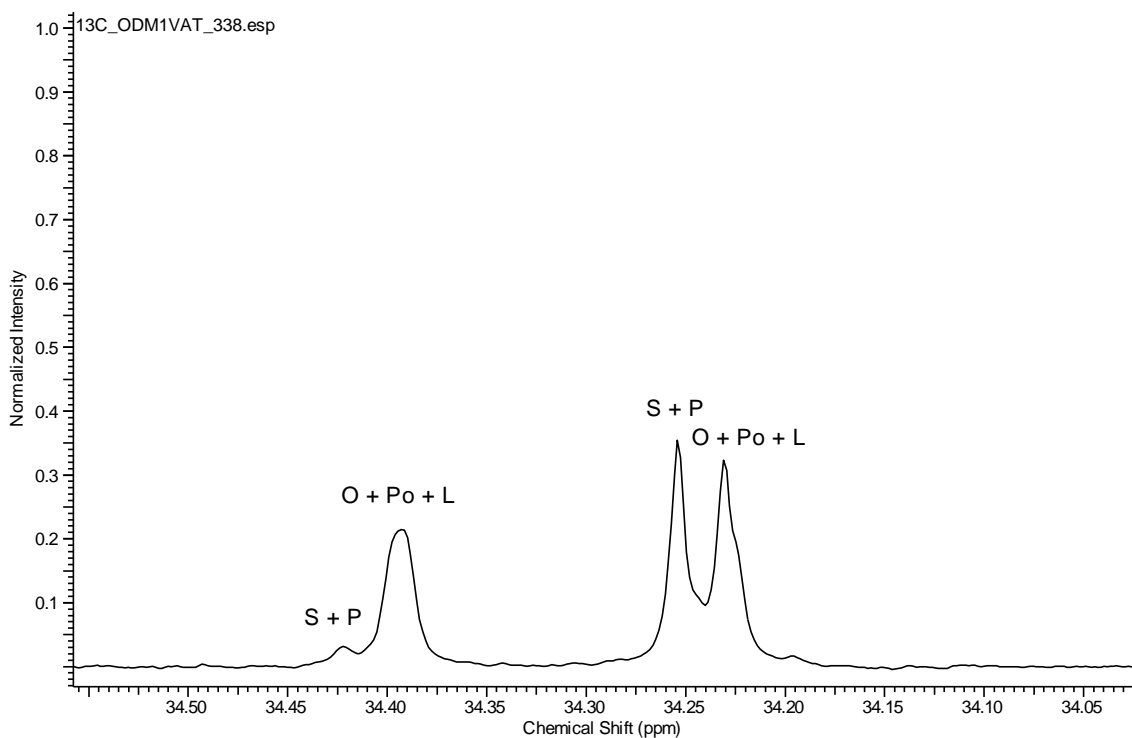


Figure 23: C_2 methyl carbon region of 600 MHz ^{13}C NMR spectra of mouse visceral fat from a 12-week-old mouse. *S*-stearate acyl chain; *P*-palmitate acyl chain; *O*-oleate acyl chain; *Po*-palmitoleate acyl chain; *L*-linoleate acyl chain.

^{13}C NMR analysis of triglyceride fatty acid enrichment from ^{13}C -enriched lipogenic substrates

For the 22 ppm region there are four peaks as we saw in Figure 22. However, a close look reveals that the chemical shift dispersion of these four peaks are identical to that observed in the standard mixture (Figure 17). Moreover, the relative intensities of the signals were similar to those of the synthetic mixture.

In the 34 ppm region (Figure 23) the signals of the mouse visceral adipose tissue triglyceride had near-identical chemical shifts and similar signal intensities to the standard mix were also found.

Finally, the 174 ppm region representing the carboxyl carbons (Figure 24), has an array of signals corresponding to different fatty acid species and their positions in the glycerol moiety. According to the literature (Gouk et al., 2012) and taking in account the data from the literature that shows a minor probability of saturated fatty acyl chains to be in the position 2 from the glycerol backbone, we can expect that the minor intensity peak (173,07 ppm) will correspond to the saturated fatty acyl chains, stearate and palmitate possibly. The signals in 173,03 and 173,04 correspond to linoleate and oleate according to the literature.

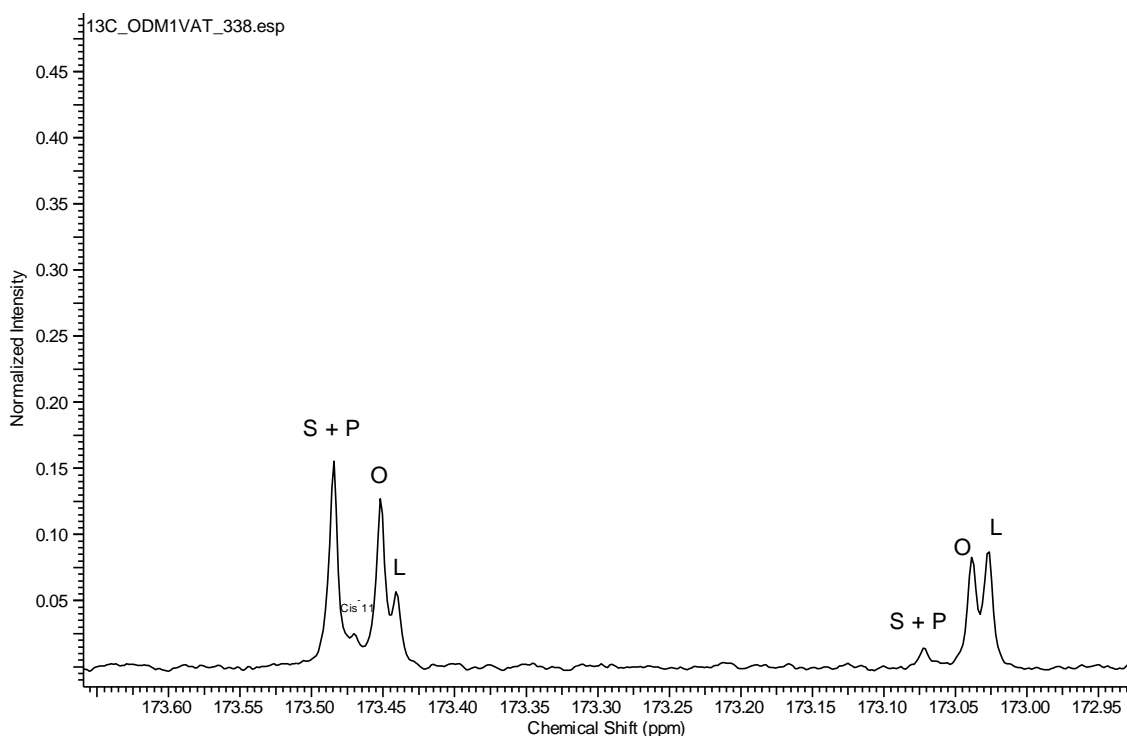


Figure 24: Carbonyl carbon region of 600 MHz ^{13}C NMR spectra of mouse visceral fat from a 12-week-old mouse. S-stearate acyl chain; P-palmitate acyl chain; O-oleate acyl chain; Po-palmitoleate acyl chain; L-linoleate acyl chain; cis-11-monoene acyl chain.

For the position 1,3 carbonyl carbons the assignments are linoleate, oleate corresponding to the lower frequencies as in the position 2 chains and then there is a small peak at 173.47 ppm which according to literature refers to a cis-11-monoene acyl

¹³C NMR analysis of triglyceride fatty acid enrichment from ¹³C-enriched lipogenic substrates

chain, which possibly will be from arachidonic acid, since the mice have this fatty acid in their lipidome in considerable amount. The last peak should correspond to the saturated species. The total fatty acid composition obtained from 3 replicates of visceral fat from mouse, according to this methodology it's presented in Table 4, and the data obtained from ACDLabs and the calculations in more detail from each sample it's present in the Annex II.

Table 4: Relative integration areas obtained with ACDLabs from the 600 MHz ¹³C NMR spectra of the mouse visceral fat.

Region (relative integration area %)	14ppm	22 ppm	34 ppm		173 ppm		Composition (mol%)	
			Position 1,3 from glycerol backbone	Position 2 from glycerol backbone	Position 1,3 from glycerol backbone	Position 2 from glycerol backbone	Position 1,3 from glycerol backbone	Position 2 from glycerol backbone
Stearate	18,93±1,77	20,77±1,43	31,38±1,86	3,58±0,35	31,31±1,10	1,88±0,17	19,85*±0,92	
Palmitate	81,07±1,77	35,84±3,22					14,23**±0,92	
Oleate		36,24±2,85	36,24±2,85					
Palmitoleate		7,15±1,04	7,15±1,04					
Linoleate		35,84±3,22	5,81±0,63	15,52±2,67	5,81±0,63	15,52±2,67		
Cis-11- monoene		ND	ND	ND	2,38±0,15	ND	2,38±0,15	ND
Total	100,00	100,00	67,35	32,65	67,60	33,19	101,17	

ND- Not detected.

^{a)} Values are mean of three replicates ± SD.

*obtained by calculating the average between the values obtained for stearate contribution.

**obtained by subtracting the average value of stearate to the value of stearate+palmitate peaks in the 34ppm and 174 ppm region.

Looking at this table it's possible to see that by some easy substitutions we can obtain the individual contributions from each fatty acid. Besides that, it's clear that the most abundant fatty acid is oleate and it becomes also clear the preference for saturated fatty acids in the external positions from the glycerol backbone and the preference for unsaturated fatty acids in the central positions.

It's also interesting note, that the unsaturated fatty acids are in similar proportions in the internal and external positions of the triglycerides although we see a 3 times bigger proportion of linoleate in the central position. This may rise questions related to the

^{13}C NMR analysis of triglyceride fatty acid enrichment from ^{13}C -enriched lipogenic substrates

conformation of the triglycerides and their specificity for the active center of enzymes related to the numerous pathways where the triglycerides are involved.

5.4 Detection of ^{13}C - ^{13}C -coupling and measurement of ^{13}C - ^{13}C coupling constants

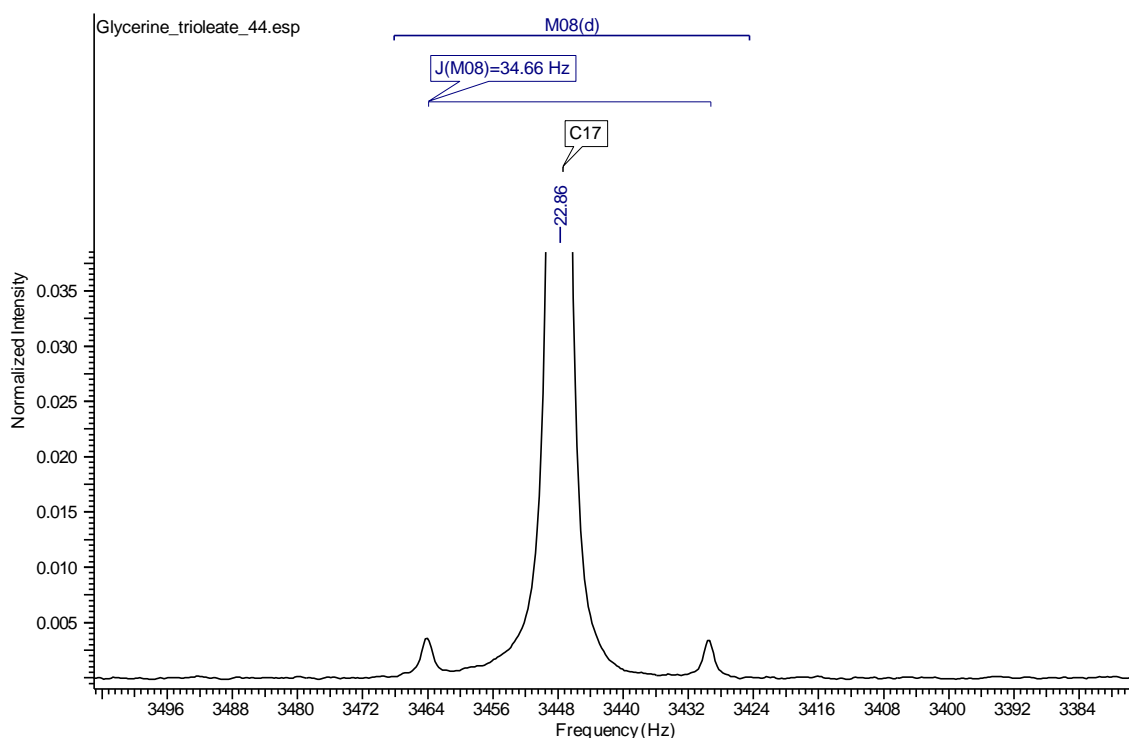


Figure 25: ^{13}C - ^{13}C coupling in the penultimate carbon from trioleate in 600 MHz ^{13}C NMR spectra.

The splitting of an observed ^{13}C signal into a doublet as the result of the presence of a neighboring ^{13}C , known as ^{13}C - ^{13}C -spin-spin coupling, is an extremely useful property for detecting enrichment from metabolic tracers. With natural abundance ^{13}C , the probability of two neighboring ^{13}C nuclei is very low, hence the characteristic doublet signal from ^{13}C - ^{13}C -spin-spin coupled nuclei is very small compared to the singlet. Nevertheless, this signal can be detected in highly concentrated samples, as shown in Figure 25 for glyceryl trioleate. In our studies, we were able to observe ^{13}C - ^{13}C -spin-spin coupled signals from concentrated solutions of glyceryl trioleate and measure the coupling constants for various carbons. This work is in the process of being extended to other single triglyceride standards such as glyceryl tripalmitate, glyceryl tristearate and glyceryl trilinoleate. Single triglyceride samples rather than standards were/are being used because the ^{13}C - ^{13}C -spin-spin coupled signals are only observable with high fatty acid concentrations (which become diluted in triglyceride mixtures). Unlike the chemical shifts, the ^{13}C - ^{13}C -coupling constants do not vary with fatty acid concentration, hence the values we get from a single fatty acid standard will be apply to that fatty acid if it is mixed with other fatty acids.

^{13}C NMR analysis of triglyceride fatty acid enrichment from ^{13}C -enriched lipogenic substrates

The importance of identifying and measuring ^{13}C - ^{13}C -spin-spin coupled signals becomes clear in metabolic studies of fatty acid synthesis from ^{13}C -enriched precursors such as $[\text{U-}^{13}\text{C}]\text{glucose}$. As shown in Figure 6, this tracer is metabolized to $[1,2\text{-}^{13}\text{C}_2]\text{acetyl-CoA}$, which is incorporated into fatty acids via *de novo* lipogenesis. As a result, each ^{13}C that was derived from the tracer is always accompanied by a neighboring ^{13}C , hence this appears as a doublet in the ^{13}C NMR spectrum. Thus, the fatty acid ^{13}C -enrichment from the tracer can be resolved from that of the background and quantified after subtracting the very small amount of naturally-occurring ^{13}C - ^{13}C -spin coupled signals. Since triglycerides derived from plant and animal tissues consist of a mixture of fatty acids, some of which can be enriched by metabolic tracers, the resulting spectrum can be highly complex. Figures 26 and 27 show regions of a ^{13}C NMR spectrum of liver triglyceride from a mouse that had been fed with a diet containing $[\text{U-}^{13}\text{C}]\text{glucose}$. Based on our studies, we were able to identify the signals corresponding to the natural abundance ^{13}C of oleate as well as the ^{13}C - ^{13}C -spin coupled signals of oleate that had been synthesized from the $[\text{U-}^{13}\text{C}]\text{glucose}$. The next step will be to identify the chemical shifts and coupling constants of the other fatty acid components in these mixtures so that all of the NMR signals are accounted for.

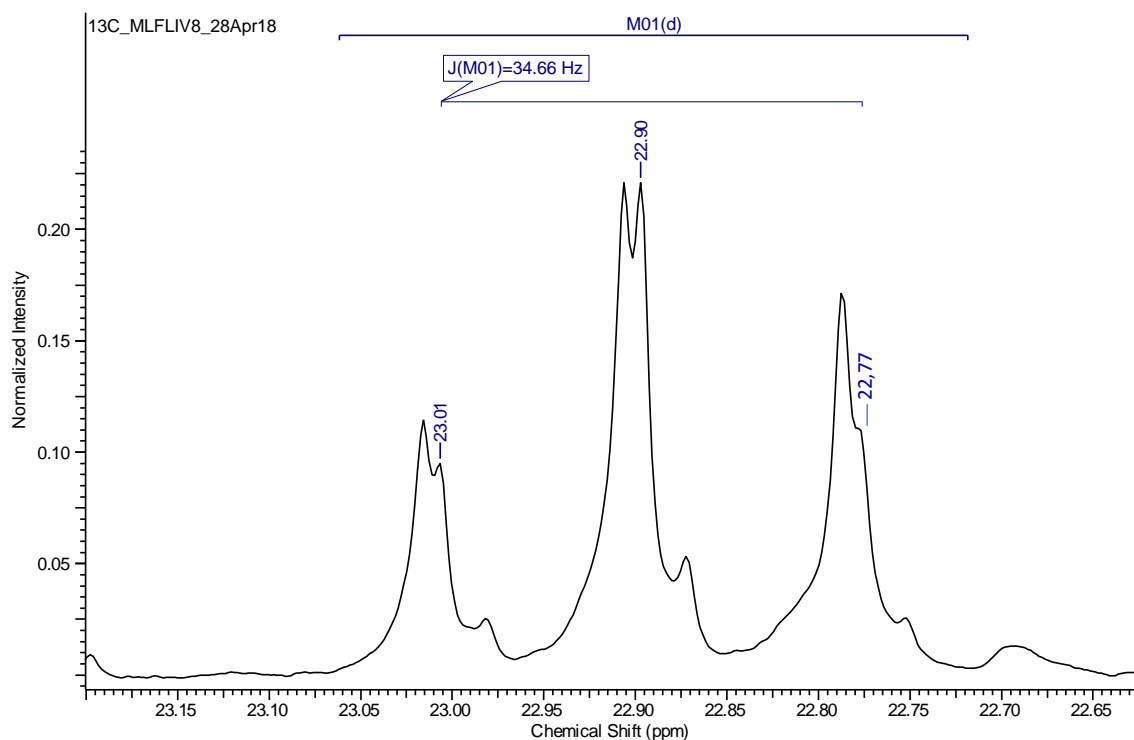


Figure 26: ^{13}C NMR spectrum of triglyceride obtained from a sample of liver tissue of mouse that had been previously fed with standard chow and $[\text{U-}^{13}\text{C}]\text{glucose}$ in the drinking water. The ^{13}C - ^{13}C coupling in the penultimate carbon of oleate is indicated.

^{13}C NMR analysis of triglyceride fatty acid enrichment from ^{13}C -enriched lipogenic substrates

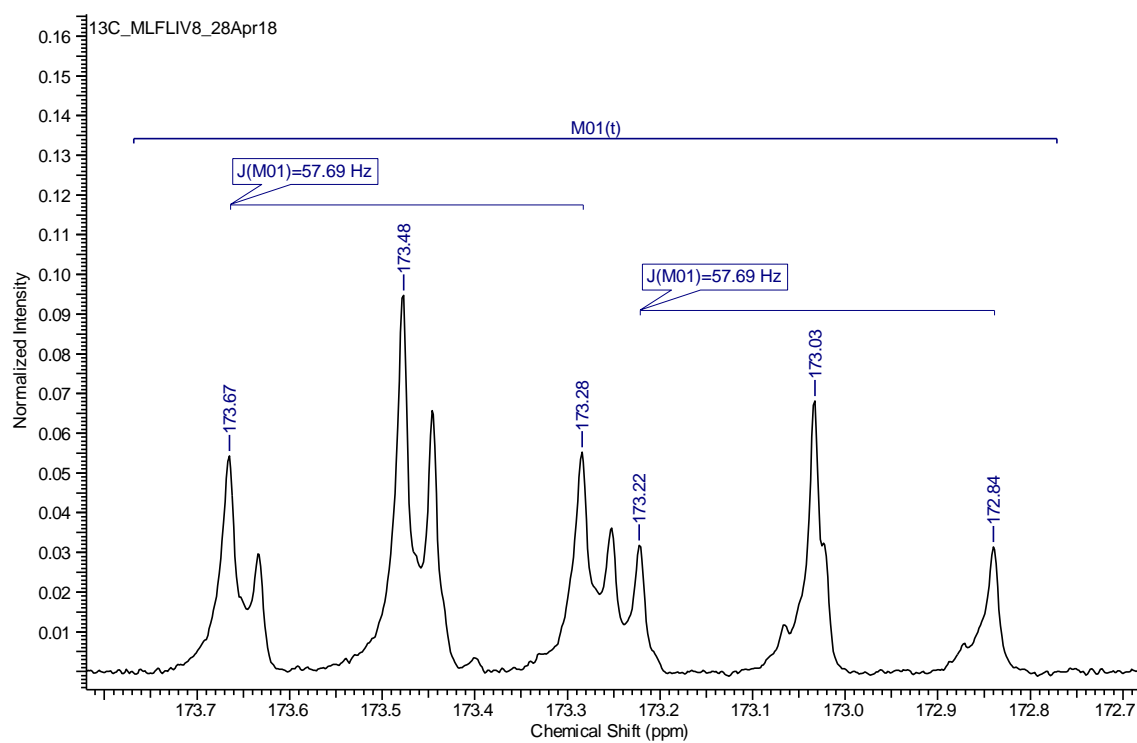


Figure 27: ^{13}C NMR spectrum of triglyceride obtained from a sample of liver tissue of mouse that had been previously fed with standard chow and $[U-^{13}\text{C}]$ glucose in the drinking water. The ^{13}C - ^{13}C coupling in the carbonyl carbon of oleate is indicated.

6 Conclusions

From the present work it's possible to affirm that ^{13}C NMR is a relatively simple method that can provide both qualitative and quantitative analyses of triglycerides after identification and assignment of individual fatty acid ^{13}C signals. For some of the carbons, chemical shift assignment has to take into account both the fatty acid species *and* its relative abundance in the sample. Among other things, this means that fatty acid signals cannot be validated by the addition of a triglyceride standard to the sample since this would alter the total concentration of that species and therefore the chemical shift would also change. This work suggests that ^{13}C NMR can be a highly effective and practical method for determining the fatty acid composition of triglycerides from living organisms. Moreover, this lipidomic information can be integrated with ^{13}C -enriched tracer studies of fatty acid biosynthesis, since the natural-abundance signals that provide the lipidomic information can be resolved from ^{13}C - ^{13}C -coupled signals arising from incorporation of a uniformly-enriched ^{13}C -substrate. This combination will prove useful in the study of diseases involving fatty acid metabolism such as Type 2 diabetes and fatty liver disease.

For future studies, will be interesting to acquire ^{13}C NMR spectra at higher fields (800 MHz) which should provide better signal dispersion and improved sensitivity, particularly for the carboxyl signals.

7 References

- Barison, A., Pereira da Silva, C. W., Campos, F. R., Simonelli, F., Lenz, C. A., & Ferreira, A. G. (2010). A simple methodology for the determination of fatty acid composition in edible oils through ¹H NMR spectroscopy. *Magnetic Resonance in Chemistry*, (June), n/a-n/a. <https://doi.org/10.1002/mrc.2629>
- Berry, S. E. E. (2009). Triacylglycerol structure and interesterification of palmitic and stearic acid-rich fats: An overview and implications for cardiovascular disease. *Nutrition Research Reviews*, 22(1), 3–17. <https://doi.org/10.1017/S0954422409369267>
- Blachier, M., Leleu, H., Peck-radosavljevic, M., Valla, D., & Roudot-thoraval, F. (2013). Special Review The burden of liver disease in Europe: A review of available epidemiological data. *Journal of Hepatology*, 58(3), 593–608. <https://doi.org/10.1016/j.jhep.2012.12.005>
- Brockhoff, H., Hoyle, R. J., & Wolmark, N. (1966). Positional distribution of fatty acids in triglycerides of animal depot fats. *Biochimica et Biophysica Acta (BBA)/Lipids and Lipid Metabolism*, 116(1), 67–72. [https://doi.org/10.1016/0005-2760\(66\)90092-0](https://doi.org/10.1016/0005-2760(66)90092-0)
- Calder, P. C. (2015). Functional Roles of Fatty Acids and Their Effects on Human Health. *Journal of Parenteral and Enteral Nutrition*, 39, 18S–32S. <https://doi.org/10.1177/0148607115595980>
- Chen, H. C., & Farese, R. V. (2002). Fatty acids, triglycerides, and glucose metabolism: Recent insights from knockout mice. *Current Opinion in Clinical Nutrition and Metabolic Care*, 5(4), 359–363. <https://doi.org/10.1097/00075197-200207000-00002>
- Evilia, R. F. (2001). Quantitative NMR spectroscopy. *Analytical Letters*, 34(13), 2227–2236. <https://doi.org/10.1081/AL-100107290>
- Fahy, E., Cotter, D., Sud, M., & Subramaniam, S. (2011). Lipid classification, structures and tools. *Biochimica et Biophysica Acta - Molecular and Cell Biology of Lipids*, 1811(11), 637–647. <https://doi.org/10.1016/j.bbalip.2011.06.009>
- Garulet, M., Pérez-Illamas, F., Pérez-ayala, M., Martínez, P., & Medina, F. S. De. (2001). Site-specific differences in the fatty acid composition of abdominal adipose tissue in an obese population from a Mediterranean area : relation with dietary fatty acids , plasma lipid profile , serum insulin , (March).
Figure 28

¹³C NMR analysis of triglyceride fatty acid enrichment from ¹³C-enriched lipogenic substrates

Gouk, S. W., Cheng, S. F., Ong, A. S. H., & Chuah, C. H. (2012). Rapid and direct quantitative analysis of positional fatty acids in triacylglycerols using ¹³C NMR. *European Journal of Lipid Science and Technology*, 114(5), 510–519. <https://doi.org/10.1002/ejlt.201100074>

Hamilton, J. G., & Comai, K. (1988). Rapid separation of neutral lipids, free fatty acids and polar lipids using prepacked silica sep-Pak columns. *Lipids*, 23(12), 1146–1149. <https://doi.org/10.1007/BF02535281>

Karantonis, H. C., Nomikos, T., & Demopoulos, C. a. (2009). Triacylglycerol metabolism. *Current Drug Targets*, 10(4), 302–319. <https://doi.org/10.2174/138945009787846443>

Keeler, J. (2002). Understanding NMR Spectroscopy. *SpringerReference*, (December), 211. https://doi.org/10.1007/SpringerReference_67582

Laposata, M. (1995). Fatty acids: Biochemistry to clinical significance. *American Journal of Clinical Pathology*, 104(2), 172–179. <https://doi.org/10.1093/ajcp/104.2.172>

Mannina, L., Luchinat, C., Patumi, M., Emanuele, M. C., Rossi, E., & Segre, A. (2000). Concentration dependence of ¹³C NMR spectra of triglycerides: implications for the NMR analysis of olive oils. *Magnetic Resonance in Chemistry*, 38(10), 886–890. [https://doi.org/10.1002/1097-458X\(200010\)38:10<886::AID-MRC738>3.0.CO;2-J](https://doi.org/10.1002/1097-458X(200010)38:10<886::AID-MRC738>3.0.CO;2-J)

MARTIN, G. E., & CROUCH, R. C. (1991). ChemInform Abstract: Inverse-Detected Two-Dimensional NMR Methods: Applications in Natural Products Chemistry. *ChemInform*, 22(31), no--no.

Miyake, Y., Yokomizo, K., & Matsuzaki, N. (1998). Determination of unsaturated fatty acid composition by high-resolution nuclear magnetic resonance spectroscopy. *Journal of the American Oil Chemists' Society*, 75(9), 1091–1094. <https://doi.org/10.1007/s11746-998-0118-4>

Sanders, F. W. B., & Griffin, J. L. (2016). De novo lipogenesis in the liver in health and disease: More than just a shunting yard for glucose. *Biological Reviews*, 91(2), 452–468. <https://doi.org/10.1111/brv.12178>

Tokunaga, T., & Okamoto, M. (2010). Recent progress in LC-NMR. *Sumitomo Chemical Co., Ltd.*, 1–10.

Vlahov, G. (1999). Application of NMR to the study of olive oils. *Progress in Nuclear Magnetic Resonance Spectroscopy - PROG NUCL MAGN RESON SPECTROS*, 35(4), 341–357. [https://doi.org/10.1016/S0079-6565\(99\)00015-1](https://doi.org/10.1016/S0079-6565(99)00015-1)

¹³C NMR analysis of triglyceride fatty acid enrichment from ¹³C-enriched lipogenic substrates

Xu, S., Jay, A., Brunaldi, K., Huang, N., & Hamilton, J. A. (2013). CD36 enhances fatty acid uptake by increasing the rate of intracellular esterification but not transport across the plasma membrane. *Biochemistry*, 52(41), 7254–7261. <https://doi.org/10.1021/bi400914c>

Annex I

Table 5: Data from the triglyceride synthetic mixture obtained with ACDLabs software.

Assignments	No.	(ppm)	(Hz)	*(ppm)	*(Hz)	Height	*Height	*FWHH	*Area	*LF	*Function	Experimental Ratios (% Sum)
CH ₃ -CH ₂ -	1	14,24	2147,7	14,24	2147,51	0,0269	0,0253	1,66	80253816	0	Gauss+Lorentz	5,18
CH ₃ -CH ₂ -	2	14,28	2153,1	14,28	2153,19	0,336	0,3443	2,03	1468107520	0,27	Gauss+Lorentz	94,82
CH ₃ -CH ₂ -	3	22,79	3437,1	22,79	3437,16	0,0636	0,0641	0,82	106890408	0,16	Gauss+Lorentz	6,46
CH ₃ -CH ₂ -	4	22,87	3449,6	22,87	3449,65	0,0405	0,0346	0,78	51511100	0	Gauss+Lorentz	3,11
CH ₃ -CH ₂ -	5	22,9	3453,6	22,9	3453,48	0,4759	0,4739	0,76	868206016	0,68	Gauss+Lorentz	52,47
CH ₃ -CH ₂ -	6	22,91	3455	22,91	3454,9	0,2856	0,2731	0,87	627039616	1	Gauss+Lorentz	37,89
1,3-OOC-CH ₂ -	7	34,24	5163,9	34,24	5164	0,3897	0,3933	1,3	1348639104	1	Gauss+Lorentz	47,80
1,3-OOC-CH ₂ -	8	34,27	5168,1	34,27	5168,23	0,1867	0,183	1,12	501192384	0,73	Gauss+Lorentz	17,76
2-OOC-CH ₂ -	9	34,41	5189,3	34,41	5189,32	0,1993	0,1963	1,34	693191296	1	Gauss+Lorentz	24,57
2-OOC-CH ₂ -	10	34,44	5193,9	34,44	5193,91	0,0894	0,0846	1,26	278621664	0,96	Gauss+Lorentz	9,87
2-OOC-CH ₂ -	11	173,06	26099,8	173,06	26099,64	0,0857	0,088	1,02	235710320	1	Gauss+Lorentz	25,47
1,3-OOC-CH ₂ -	12	173,09	26105,1	173,09	26105,2	0,0387	0,0388	1,02	9,34E+07	0,61	Gauss+Lorentz	10,09
2-OOC-CH ₂ -	13	173,47	26162,1	173,47	26162,04	0,1613	0,164	1,02	440659744	1	Gauss+Lorentz	47,62
1,3-OOC-CH ₂ -	14	173,51	26167,7	173,51	26167,74	0,0751	0,0725	1	155634640	0,32	Gauss+Lorentz	16,82

Annex II

Table 6: Data from the mice visceral fat #1 obtained with ACDLabs software

¹³ C ODMIVAT	338CDC13	No.	(ppm)	(Hz)	*(ppm)	*(Hz)	Height	*Height	*FWHH	*Area	*JF	*Function	Experimental Ratios (%)	Total Area of the peaks
Stearate		1	14,27	2152,5	14,27	2152,45	0,1285	0,1213	1,43	671455616	1	Gauss+Lorentz	21,33	3147526016
Others		2	14,31	2158,7	14,31	2158,92	0,2919	0,2977	2,39	2476070400	0,63	Gauss+Lorentz	78,67	3147526016
Stearate		3	22,78	3435,3	22,78	3435,35	0,1897	0,1983	1,01	765924864	0,95	Gauss+Lorentz	22,79	3361262224
Palmitoleate		4	22,86	3447,8	22,86	3447,91	0,0614	0,0582	1,02	229619088	1	Gauss+Lorentz	6,83	3361262224
Oleate		5	22,89	3451,8	22,89	3451,73	0,3541	0,3449	0,98	1306060288	0,98	Gauss+Lorentz	38,86	3361262224
Palmitate+Linolate		6	22,9	3453,2	22,9	3453,2	0,3271	0,3079	0,91	1059657984	0,93	Gauss+Lorentz	31,53	3361262224
Oleate+Linolate+Palmitoleate		7	34,23	5162,6	34,23	5162,42	0,323	0,3059	1,75	2074573440	1	Gauss+Lorentz	37,44	5541680640
Stearate+Palmitate		8	34,25	5166,1	34,25	5166,06	0,3543	0,3364	1,27	1622290944	0,94	Gauss+Lorentz	29,27	5541680640
Oleate+Linolate+Palmitoleate		9	34,39	5187	34,39	5187,13	0,2142	0,224	2,44	1673455360	0,24	Gauss+Lorentz	30,20	5541680640
Stearate+Palmitate		10	34,42	5191,4	34,42	5191,38	0,0313	0,0261	1,94	171360896	0,54	Gauss+Lorentz	3,09	5541680640
Linoleate		11	173,03	26095,2	173,03	26095,3	0,0866	0,0854	1,01	290346144	0,52	Gauss+Lorentz	15,30	1897284794
Oleate+Palmitoleate		12	173,04	26097,1	173,04	26097,02	0,0827	0,0796	1,14	3,19E+08	0,68	Gauss+Lorentz	16,84	1897284794
Stearate+Palmitate		13	173,07	26102,2	173,07	26102,19	0,014	0,014	0,7	33213974	0,52	Gauss+Lorentz	1,75	1897284794
Linoleate		14	173,44	26157,8	173,44	26157,66	0,0568	0,0446	0,96	126945856	0,15	Gauss+Lorentz	6,69	1897284794
Oleate+Palmitoleate		15	173,45	26159,4	173,45	26159,37	0,1271	0,1268	1,02	502949504	1	Gauss+Lorentz	26,51	1897284794
Cis-11-Monoene		16	173,47	26162,2	173,47	26162,16	0,0251	0,0132	1,13	42285316	0,03	Gauss+Lorentz	2,23	1897284794
Stearate+Palmitate		17	173,48	26164,3	173,48	26164,36	0,1555	0,1541	0,99	582111104	0,94	Gauss+Lorentz	30,68	1897284794

¹³C NMR analysis of triglyceride fatty acid enrichment from ¹³C-enriched lipogenic substrates

Table 7: Data from the mice visceral fat #2 obtained with ACDLabs software

¹³ C	ODM/VAT_339CDCI3	No.	(ppm)	(Hz)	*(ppm)	*(Hz)	Height	*Height	*FWHH	*Area	*LF	*Function	Experimental Ratios (%)	Total Area of the peaks
	Stearate	1	14,27	2151,5	14,27	2151,58	0,1158	0,1091	1,4	6,98E+08	0,86	Gauss+Lorentz	18,33	3807161344
	Others	2	14,31	2158,5	14,31	2158,1	0,2986	0,3016	2,43	3,11E+09	0,62	Gauss+Lorentz	81,67	3807161344
	Stearate	3	22,77	3434,8	22,78	3434,91	0,1739	0,1795	1,01	8,07E+08	0,8	Gauss+Lorentz	19,92	4053097920
	Palmitoleate	4	22,86	3447,6	22,86	3447,47	0,079	0,0738	1,1	3,46E+08	0,64	Gauss+Lorentz	8,55	4053097920
	Oleate	5	22,88	3451,3	22,88	3451,27	0,317	0,2853	1,01	1,31E+09	0,86	Gauss+Lorentz	32,28	4053097920
	Palmitate+Linolate	6	22,89	3452,7	22,89	3452,77	0,3743	0,3503	0,99	1,59E+09	0,88	Gauss+Lorentz	39,25	4053097920
	Oleate+Linoleate+Palmitoleate	7	34,22	5161,7	34,22	5161,46	0,2822	0,2641	1,79	2,21E+09	0,95	Gauss+Lorentz	33,54	6588685584
	Stearate+Palmitate	8	34,25	5164,9	34,25	5165,06	0,3699	0,3583	1,35	2,23E+09	0,89	Gauss+Lorentz	33,79	6588685584
	Oleate+Linoleate+Palmitoleate	9	34,39	5186,1	34,39	5186,19	0,196	0,2056	2,48	1,9E+09	0,23	Gauss+Lorentz	28,86	6588685584
	Stearate+Palmitate	10	34,42	5190,5	34,42	5190,42	0,0405	0,0354	1,89	2,51E+08	0,25	Gauss+Lorentz	3,81	6588685584
	Linoleate	11	173,02	26093,6	173,02	26093,52	0,076	0,0747	1,32	4,5E+08	0,88	Gauss+Lorentz	18,90	2383255552
	Oleate+Palmitoleate	12	173,03	26095,2	173,03	26095,27	0,0719	0,0643	1,13	2,85E+08	0,38	Gauss+Lorentz	11,98	2383255552
	Stearate+Palmitate	13	173,06	26100,3	173,06	26100,33	0,0147	0,0147	0,7	42048560	0,5	Gauss+Lorentz	1,76	2383255552
	Linoleate	14	173,43	26155,9	173,43	26155,93	0,0459	0,0459	0,7	1,31E+08	0,5	Gauss+Lorentz	5,50	2383255552
	Oleate+Palmitoleate	15	173,44	26157,3	173,44	26157,27	0,0947	0,0899	1,77	7,5E+08	0,98	Gauss+Lorentz	31,47	2383255552
	Cis-11-Monoene									ND				
	Stearate+Palmitate	16	173,47	26162,2	173,47	26162,31	0,1328	0,1332	1,29	7,24E+08	0,59	Gauss+Lorentz	30,39	2383255552

¹³C NMR analysis of triglyceride fatty acid enrichment from ¹³C-enriched lipogenic substrates

Table 8: Data from the mice visceral fat #3 obtained with ACDLabs software

¹³ C ODMSVAT_366DCI3	No.	(ppm)	(Hz)	*(ppm)	*(Hz)	Height	*Height	*FWHH	*Area	*LF	*Function	Experimental Ratios (%)	Total area of the peaks
Stearate	1	14,27	2152,2	14,27	2152,12	0,1116	0,1074	1,39	6,65E+08	0,96	Gauss+Lorentz	17,13	3881984384
Others	2	14,32	2159	14,31	2158,64	0,3018	0,528	1,36	3,22E+09	0,99	Gauss+Lorentz	82,87	3881984384
Stearate	3	22,78	3435,3	22,78	3435,22	0,1715	0,1721	1,02	7,53E+08	0,85	Gauss+Lorentz	19,62	3837766592
Palmitoleate	4	22,86	3447,8	22,86	3447,78	0,0645	0,056	1,1	2,33E+08	0,43	Gauss+Lorentz	6,07	3837766592
Oleate	5	22,89	3451,6	22,89	3451,58	0,3646	0,3363	1	1,44E+09	0,84	Gauss+Lorentz	37,58	3837766592
Palmitate+Linolate	6	22,9	3453	22,9	3453,08	0,3351	0,32	1,02	1,41E+09	0,85	Gauss+Lorentz	36,73	3837766592
Oleate+Linolate+Palmitoleate	7	34,23	5162,4	34,23	5162,25	0,2853	0,2627	1,81	2,12E+09	0,97	Gauss+Lorentz	36,93	5749472640
Stearate+Palmitate	8	34,25	5165,9	34,25	5165,89	0,3269	0,3079	1,31	1,79E+09	0,94	Gauss+Lorentz	31,07	5749472640
Oleate+Linolate+Palmitoleate	9	34,39	5187	34,39	5187,03	0,1844	0,1915	2,42	1,62E+09	0,19	Gauss+Lorentz	28,14	5749472640
Stearate+Palmitate	10	34,42	5191,2	34,42	5191,17	0,0307	0,0272	2,07	2,22E+08	0,55	Gauss+Lorentz	3,85	5749472640
Linoleate	11	173,03	26096,1	173,03	26096,02	0,0702	0,0665	1,03	2,42E+08	0,23	Gauss+Lorentz	12,36	1958393500
Oleate+Palmitoleate	12	173,04	26097,8	173,04	26097,74	0,0799	0,0799	1,1	3,64E+08	0,72	Gauss+Lorentz	18,56	1958393500
Stearate+Palmitate	13	173,08	26102,9	173,08	26102,89	0,0153	0,0153	0,7	41401056	0,5	Gauss+Lorentz	2,11	1958393500
Linoleate	14	173,45	26158,5	173,45	26158,54	0,0422	0,0318	0,9	1,02E+08	0,27	Gauss+Lorentz	5,23	1958393500
Oleate+Palmitoleate	15	173,46	26160,1	173,46	26160,21	0,1098	0,1101	1,04	5,16E+08	1	Gauss+Lorentz	26,34	1958393500
Cis-11-Monoene	16	173,48	26163,1	173,48	26163,14	0,0182	0,0182	0,7	49378044	0,5	Gauss+Lorentz	2,52	1958393500
Stearate+Palmitate	17	173,49	26165,2	173,49	26165,23	0,1423	0,1417	1,01	6,44E+08	0,99	Gauss+Lorentz	32,86	1958393500